COMMUN. MATH. SCI.
Vol. 16, No. 6, pp. 1635–1658

DIRECT AND INVERSE ELASTIC SCATTERING FROM A LOCALLY PERTURBED ROUGH SURFACE*

GUANGHUI HU†, XIAOKAI YUAN‡, AND YUE ZHAO§

Abstract. This paper is concerned with time-harmonic elastic scattering from a locally perturbed rough surface in two dimensions. We consider a rigid scattering interface given by the graph of a one-dimensional Lipschitz function which coincides with the real axis in the complement of some compact set. Given the incident field and the scattering interface, the direct problem is to determine the field distribution, whereas the inverse problem is to determine the shape of the interface from the measurement of the field on an artificial boundary in the upper half-plane. We propose a symmetric coupling method between finite element and boundary integral equations to show uniqueness and existence of weak solutions. The synthetic data is computed via the finite element method with the Perfectly Matched Layer (PML) technique. To investigate the inverse problem, we derive the domain derivatives of the field with respect to the scattering interface. An iterative continuation method with multi-frequency data is used for recovering the unknown scattering interface.

Keywords. Linear elasticity; Fredholm alternative; half-plane; rigid surface; inverse scattering; multi-frequency data; local perturbation.

AMS subject classifications. 35A15; 74B05; 74J20; 78A46.

1. Introduction

The scattering problems in a locally perturbed half-space have attracted much attention over the last twenty years. Such problems are also referred to as cavity scattering problems in the literature. They have many applications in remote sensing, geophysics, outdoor sound propagation, radar techniques and so on. Consequently, significant progress has been made concerning the mathematical analysis and the numerical approximation of the acoustic and electromagnetic scattering problems modeled by the Helmholtz and Maxwell's equations. We refer to [6–8, 20, 25–28, 32–34] for the variational and integral equation methods adopted to reduce the unbounded physical domain to a truncated computational domain. However, little analysis for the Navier equation has been carried out. This paper is devoted to direct and inverse time-harmonic elastic scattering from a locally perturbed rigid rough surface in two dimensions. The relevant phenomena for elastic wave propagation in a perturbed half-plane have many applications in geophysics, ocean acoustics and seismology (see e.g., [1,2,31] and the references therein).

In contrast to acoustic and electromagnetic scattering problems, it seems impossible to derive a transparent boundary condition (or the so-called non-reflecting boundary operator) for Kupradze radiation solutions of the Navier equation in a half-space. This is essentially due to the lack of an analogous reflection principle for the Navier equation across a rigid flat surface. In the case of Helmholtz and Maxwell equations, the reflection principles give rise to a serious expansion of half-space Sommerfeld radiation solutions satisfying the Dirichlet or Neumann boundary condition on the ground plane. In this paper, we propose a variational approach in a truncated bounded domain coupled with

*Received: January 7, 2018; Accepted (in revised form): June 8, 2018. Communicated by Liliana Borcea.

†Beijing Computational Science Research Center, Beijing 100193, China (hu@csrc.ac.cn).

‡Department of Mathematics, Purdue University, West Lafayette, Indiana 47907, USA (yuan170@math.purdue.edu).

§Corresponding author: School of Mathematics and Statistics, Central China Normal University, Wuhan 430079, China (zhaoyueccnu@163.com).

the Dirichlet-to-Neumann map derived from an integral representation of the outgoing radiation solutions. The Dirichlet Green's tensor in a half-plane is used as the kernel of the single and double layer operators. Such kind of coupling scheme is closest to the lines of [8, 19, 26]. It can be used to handle various boundary value problems in a locally perturbed half-space, provided the Green's function to the unperturbed problem fulfills the outgoing radiation condition; see [9] for the treatment of the Robin boundary condition and transmission conditions for the Helmholtz equation. We prove that the resulting sesquilinear form is strongly elliptic and thus the Fredholm theory can be applied to yield well-posedness. It should be noted that an efficient calculation of the half-space's Green's tensor is not trivial. Hence, numerical approximations based on the proposed coupling scheme is time-consuming. Instead, the finite element method with the Perfectly Matched Layer (PML) technique will be employed as a forward solver.

The analysis for locally perturbed rough surfaces has significantly simplified the arguments for general unbounded rough surfaces (see e.g., [4, 5, 12, 14]). In the latter case, the perturbed field is required to fulfill a weak Upward Propagating Radiation Condition (UPRC) in the half-space. Our solvability result shows that, in the locally perturbed case, the perturbed wave field can be uniquely decomposed into the sum of an outgoing plane wave (i.e., the reflected wave) and a Sommerfeld radiation wave (i.e., the scattered wave), both of which satisfy the UPRC. Further, the numerical approximation can be rigorously confined to a truncated bounded domain in the locally perturbed case, which simplifies the analysis and calculation for general rough surfaces. Variational approach for periodic rigid surfaces was established in [15, 16].

The second half of this paper is concerned with the inverse problem of reconstructing the shape of the scattering interface from near-field measurements of plane incident waves incited at one or multiple frequencies. Relying on the variational arguments presented in the first half and those in [18] and [21], we derive the Fréchet derivative of the solution operator with respect to the scattering surface. A different approach based on the integral equation was used in electromagnetism [30] and in elasticity [13, 23]. The shape derivative can be used to design an iterative continuation approach for shape recovery from the data of several incident frequencies. At each iteration step, the forward problem needs to be solved and the correctness of the parameters needs to be evaluated. Various examples are presented to show the validity and accuracy of our inversion algorithms. We refer to [10, 11, 34] for similar iterative approaches using acoustic multi-frequency data for imaging a locally perturbed rough surface.

The Navier equation has a more complex form than the Helmholtz equation, because it accounts for both longitudinal (pressure) and transverse (shear) motions which propagate at different wave speeds but are coupled together at the boundary of the rigid body. As can be seen from this paper, the analysis and numerics for this vectorial equation are more difficult than the scalar equations. We summarize the differences of our article with the recent publication [24] as follows. First, one-dimensional periodic surfaces are reconstructed in [24] from near-field data, whereas the perturbed section of a straight line is retrieved within this paper. There are fundamental differences between the two mathematical models, for instance, the Rayleigh Expansion Radiation Condition for periodic surfaces is much different from the outgoing radiation condition for locally perturbed rough surfaces. Second, the arguments of [24] are based on a transformed field expansion approach. The inversion scheme is applicable to periodic surfaces with a sufficiently small height, although it requires the data of one incoming wave only. On the other hand, the positions for measuring near-field data required by [24] should be sufficiently close to the real surface. In this paper, the height of the locally per-

turbed part can be arbitrarily large in theory and the initial guess is not necessarily good enough. However, the near-field data of this paper are incited at multi-frequencies, much more than the data of [24]. The domain-derivative method used in our paper also differs from that of [24].

The remaining part of this paper is organized as follows. We formulate the forward scattering problem in Section 2 and present the solvability results in Section 3. Section 4 is devoted to the proof of the Fréchet derivative and the presentation of our inversion algorithms. Numerical tests will be reported in Section 5. Concluding remarks will be presented in the last section.

2. Problem formulation

Consider a two-dimensional locally perturbed half-plane $\Gamma_f = \{\boldsymbol{x} \in \mathbb{R}^2 : x_2 = f(x_1), x_1 \in \mathbb{R}\}$, where f is a Lipschitz continuous function and is assumed to satisfy $f(x_1) = 0$ when $|x_1| > R$ for some $R > 0$. This means that Γ_f is a local perturbation of the straight line $\Gamma_0 = \{\boldsymbol{x} \in \mathbb{R}^2 : x_2 = 0\}$, since it coincides with Γ_0 in $\{\boldsymbol{x} = (x_1, x_2) \in \Gamma_f : |x_1| > R\}$; see Figure 2.1. Denote by $\Omega = \{\boldsymbol{x} \in \mathbb{R}^2 : x_2 > f(x_1), x_1 \in \mathbb{R}\}$ the space above Γ_f, which is filled with a homogeneous and isotropic elastic medium. Set $\Lambda_R := \Gamma_f \cap \{\boldsymbol{x} : |x_1| \le R\}$, which contains the perturbed part of the straight line Γ_0. Denote by $\Omega_R = \{\boldsymbol{x} \in \Omega : |\boldsymbol{x}| < R\}$ the truncated bounded domain, and by $B_R^+ = \{\boldsymbol{x} \in \mathbb{R}^2 : |\boldsymbol{x}| < R,\ x_2 > 0\}$ the upper half-circle. Let $S_R = \{\boldsymbol{x} \in \Omega : |\boldsymbol{x}| = R\}$ and denote by $\boldsymbol{\nu}$ the unit normal vector on S_R, pointing into the exterior of Ω_R. Obviously, $\partial\Omega_R = \Lambda_R \cup S_R$.

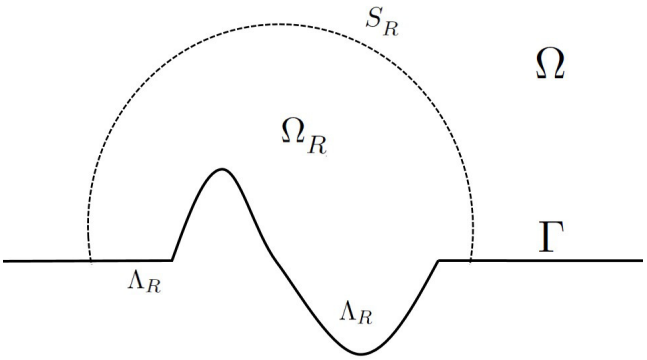

FIG. 2.1. *Geometry settings for elastic scattering from a locally perturbed half-plane.*

Let $\boldsymbol{u}^{\text{in}}$ be a time-harmonic plane wave which is incident on the scattering surface Γ_f from above in Ω. More explicitly, $\boldsymbol{u}^{\text{in}}$ is allowed to be a general elastic plane wave of the form

$$\boldsymbol{u}^{\text{in}} = c_1 \boldsymbol{u}_{\text{p}}^{\text{in}} + c_2 \boldsymbol{u}_{\text{s}}^{\text{in}}, \quad c_1, c_2 \in \mathbb{C}, \tag{2.1}$$

where $\boldsymbol{u}_{\text{p}}^{\text{in}}$ is the compressional plane wave of the form

$$\boldsymbol{u}_{\text{p}}^{\text{in}} = [\sin\theta, -\cos\theta]^\top e^{\mathrm{i}\kappa_1(x_1 \sin\theta - x_2 \cos\theta)}$$

and $\boldsymbol{u}_{\text{s}}^{\text{in}}$ is the shear plane wave

$$\boldsymbol{u}_{\text{s}}^{\text{in}} = [\cos\theta, \sin\theta]^\top e^{\mathrm{i}\kappa_2(x_1 \cos\theta + x_2 \sin\theta)},$$

where $\theta \in (-\pi/2, \pi/2)$ is the incident angle, and

$$\kappa_1 = \omega/\sqrt{\lambda+2\mu}, \quad \kappa_2 = \omega/\sqrt{\mu} \tag{2.2}$$

are the compressional and shear wavenumbers, respectively. Here $\omega > 0$ is the angular frequency, λ and μ are the Lamé constants satisfying $\mu > 0$ and $\lambda + \mu > 0$ which implies that $\kappa_1 < \kappa_2$. It can be verified that the incident field $\boldsymbol{u}^{\text{in}}$ satisfies the two-dimensional Navier equation:

$$\mu \Delta \boldsymbol{u}^{\text{in}} + (\lambda+\mu)\nabla\nabla\cdot\boldsymbol{u}^{\text{in}} + \omega^2 \boldsymbol{u}^{\text{in}} = 0 \quad \text{in } \Omega. \tag{2.3}$$

The displacement of the total field $\boldsymbol{u}$ also satisfies the same Navier equation:

$$\mu \Delta \boldsymbol{u} + (\lambda+\mu)\nabla\nabla\cdot\boldsymbol{u} + \omega^2 \boldsymbol{u} = 0 \quad \text{in } \Omega. \tag{2.4}$$

In this paper, we assume that Γ_f is a rigid impenetrable interface, that is,

$$\boldsymbol{u} = 0 \quad \text{on } \Gamma_f. \tag{2.5}$$

Due to the local perturbation, the total field $\boldsymbol{u}$ can be decomposed into three parts: the incident field $\boldsymbol{u}^{\text{in}}$, the reflected wave $\boldsymbol{u}^{\text{re}}$, and the scattered field $\boldsymbol{u}^{\text{sc}}$:

$$\boldsymbol{u} = \boldsymbol{u}^{\text{in}} + \boldsymbol{u}^{\text{re}} + \boldsymbol{u}^{\text{sc}},$$

where $\boldsymbol{u}^{\text{re}}$ is the reflected field solving the unperturbed scattering problem

$$\begin{aligned} \mu \Delta \boldsymbol{u}^{\text{re}} + (\lambda+\mu)\nabla\nabla\cdot\boldsymbol{u}^{\text{re}} + \omega^2 \boldsymbol{u}^{\text{re}} = 0 \quad &\text{in} \quad x_2 > 0, \\ \boldsymbol{u}^{\text{re}} + \boldsymbol{u}^{\text{in}} = 0 \quad &\text{on} \quad x_2 = 0, \end{aligned}$$

and $\boldsymbol{u}^{\text{sc}}$ satisfies the outgoing Kupradze radiation condition (see Definition 2.1 below). It should be remarked that the reflected field $\boldsymbol{u}^{\text{re}}$ does not fulfill the outgoing Kupradze radiation condition. Enforcing the Upward Propagating Radiation Condition (see [12, 14]) on $\boldsymbol{u}^{\text{re}}$ in the half-plane $x_2 > 0$, we may get a unique solution of $\boldsymbol{u}^{\text{re}}$. More explicitly, the reference field $\boldsymbol{u}_0 := \boldsymbol{u}^{\text{in}} + \boldsymbol{u}^{\text{re}}$ takes the form

$$\boldsymbol{u}_0(\boldsymbol{x}) = (c_1/\kappa_1)\boldsymbol{U}_{\text{p}}(\boldsymbol{x}) + (c_2/\kappa_2)\boldsymbol{U}_{\text{s}}(\boldsymbol{x}), \tag{2.6}$$

where c_1 and c_2 are the coefficients attached to the incident plane pressure and shear waves in (2.1), respectively, and

$$\begin{aligned} \boldsymbol{U}_{\text{p}}(\boldsymbol{x}) = &\begin{bmatrix} \alpha_{\text{p}} \\ -\beta_{\text{p}} \end{bmatrix} e^{\text{i}(\alpha_{\text{p}} x_1 - \beta_{\text{p}} x_2)} - \frac{\alpha_{\text{p}}^2 - \beta_{\text{p}}\eta_{\text{p}}}{\alpha_{\text{p}}^2 + \beta_{\text{p}}\eta_{\text{p}}} \begin{bmatrix} \alpha_{\text{p}} \\ \beta_{\text{p}} \end{bmatrix} e^{\text{i}(\alpha_{\text{p}} x_1 + \beta_{\text{p}} x_2)} \\ &- \frac{2\alpha_{\text{p}}\beta_{\text{p}}}{\alpha_{\text{p}}^2 + \beta_{\text{p}}\eta_{\text{p}}} \begin{bmatrix} \eta_{\text{p}} \\ -\alpha_{\text{p}} \end{bmatrix} e^{\text{i}(\alpha_{\text{p}} x_1 + \eta_{\text{p}} x_2)}, \\ \boldsymbol{U}_{\text{s}}(\boldsymbol{x}) = &\begin{bmatrix} \beta_{\text{s}} \\ \alpha_{\text{s}} \end{bmatrix} e^{\text{i}(\alpha_{\text{s}} x_1 - \beta_{\text{s}} x_2)} - \frac{\beta_{\text{s}}\eta_{\text{s}} - \alpha_{\text{s}}^2}{\alpha_{\text{s}}^2 + \beta_{\text{s}}\eta_{\text{s}}} \begin{bmatrix} \beta_{\text{s}} \\ -\alpha_{\text{s}} \end{bmatrix} e^{\text{i}(\alpha_{\text{s}} x_1 + \beta_{\text{s}} x_2)} \\ &- \frac{2\alpha_{\text{s}}\beta_{\text{s}}}{\alpha_{\text{s}}^2 + \beta_{\text{s}}\eta_{\text{s}}} \begin{bmatrix} \alpha_{\text{s}} \\ \eta_{\text{s}} \end{bmatrix} e^{\text{i}(\alpha_{\text{s}} x_1 + \eta_{\text{s}} x_2)}, \end{aligned}$$

with

$$\alpha_{\text{p}} = \kappa_1 \sin\theta, \quad \beta_{\text{p}} = \kappa_1 \cos\theta, \quad \eta_{\text{p}} = \sqrt{\kappa_2^2 - \alpha_{\text{p}}^2},$$

$$\alpha_{\mathrm{s}}=\kappa_2\sin\theta,\quad \beta_{\mathrm{s}}=\kappa_2\cos\theta,\quad \eta_{\mathrm{s}}=\sqrt{\kappa_1^2-\alpha_{\mathrm{s}}^2}.$$

The scattered field $\boldsymbol{u}^{\mathrm{sc}}$ also satisfies the Navier equation

$$\mu\Delta\boldsymbol{u}^{\mathrm{sc}}+(\lambda+\mu)\nabla\nabla\cdot\boldsymbol{u}^{\mathrm{sc}}+\omega^2\boldsymbol{u}^{\mathrm{sc}}=0\quad\text{in }\Omega. \tag{2.7}$$

Let $\boldsymbol{w}=[w_1,w_2]^\top$ be a vector function and let w be a scalar function. Introduce the two dimensional curl operators

$$\operatorname{curl}\boldsymbol{w}:=\partial_1 w_2-\partial_2 w_1,\quad \mathbf{curl}\,w:=[\partial_y w,-\partial_x w]^\top.$$

By Helmholtz decomposition, any solution of (2.7) can be split into its compressional and shear parts:

$$\boldsymbol{u}^{\mathrm{sc}}=\nabla\phi_1+\mathbf{curl}\,\phi_2, \tag{2.8}$$

where $\phi_j, j=1,2$ are scalar potential functions satisfying the Helmholtz equations

$$\Delta\phi_j+\kappa_j^2\phi_j=0. \tag{2.9}$$

We require ϕ_j to satisfy the Sommerfeld radiation condition in the half-plane:

$$\lim_{\rho\to\infty}\rho^{1/2}(\partial_\rho\phi_j-\mathrm{i}\kappa_j\phi_j)=0,\quad \rho=|\boldsymbol{x}|,\quad \boldsymbol{x}\in\{|\boldsymbol{x}|>R\}\cap\mathbb{R}^2_+. \tag{2.10}$$

The above asymptotics lead to the far-field data ϕ_j^∞ of ϕ_j $(j=1,2)$:

$$\phi_j(\boldsymbol{x})=\frac{e^{i\kappa_j\rho}}{\sqrt{\rho}}\left\{\phi_j^\infty(\hat{\boldsymbol{x}})+O(1/\rho)\right\},\qquad\text{as}\quad \rho=|\boldsymbol{x}|\to\infty. \tag{2.11}$$

Denote by Φ_1^∞ and Φ_2^∞ the far-field patterns of $\nabla\phi_1$ and $\mathbf{curl}\,\phi_2$, respectively. Then the far-field pattern of $\boldsymbol{u}^{\mathrm{sc}}$ is defined as the sum of Φ_1^∞ and Φ_2^∞.

DEFINITION 2.1. *The vector $\boldsymbol{u}^{sc}$, which is a solution to the Navier Equation (2.7) is said to satisfy the half-plane Kupradze radiation condition if its compressional part ϕ_1 and shear part ϕ_2 satisfy (2.10).*

Given the incident field $\boldsymbol{u}^{\mathrm{in}}$ and the interface Γ_f, the direct (forward) scattering problem is to determine the displacement of the total field $\boldsymbol{u}$. The inverse problem is to determine the perturbed part Λ_R from the boundary measurement of the displacement $\boldsymbol{u}$ on S_R incited by one or several incident fields.

To investigate both direct and inverse problems, we need some functional spaces as follows. Define the Sobolev space

$$H^1_{\Lambda_R}(\Omega_R)=\{u\in H^1(\Omega_R):u=0\text{ on }\Lambda_R\},$$

which is equipped with the usual H^1-norm

$$\|u\|_{1,\Omega_R}=\Big(\int_{\Omega_R}|\nabla u|^2+|u|^2\mathrm{d}\boldsymbol{x}\Big)^{1/2}.$$

Let $X_R=H^1_{\Lambda_R}(\Omega_R)^2=H^1_{\Lambda_R}(\Omega_R)\times H^1_{\Lambda_R}(\Omega_R)$ be a Cartesian product space which is equipped with the norm:

$$\|\boldsymbol{u}\|_{X_R}=(\|u_1\|^2_{1,\Omega_R}+\|u_2\|^2_{1,\Omega_R})^{1/2}.$$

Denote by $X_R^{-1}=H_{\Lambda_R}^{-1}(\Omega_R)\times H_{\Lambda_R}^{-1}(\Omega_R)$ the dual space of X_R, where $H_{\Lambda_R}^{-1}(\Omega_R)$ is the dual space of $H_{\Lambda_R}^{1}(\Omega_R)$. Introduce the Sobolev spaces on an open arc (see e.g., [29]):

$$H^{1/2}(S_R)^2:=\{u|_{S_R}:u\in H^{1/2}(\partial\Omega_R)^2\},$$
$$\tilde{H}^{1/2}(S_R)^2:=\{u\in H^{1/2}(\partial\Omega_R)^2:\mathrm{supp}(u)\subset S_R\}.$$

Then we denote by $H^{-1/2}(S_R)^2$ the dual space of $\tilde{H}^{1/2}(S_R)^2$, and by $\tilde{H}^{-1/2}(S_R)^2$ the dual space of $H^{1/2}(S_R)^2$.

3. Direct scattering

In this section, we prove that the direct scattering problem admits a unique weak solution in X_R. We propose a variational formulation in Ω_R coupled with a Dirichlet-to-Neumann map derived from the integral representation of the scattered field $\boldsymbol{u}^{\mathrm{sc}}$ in $\{\boldsymbol{x}\in\Omega:|\boldsymbol{x}|>R\}$.

We begin by introducing the free space Green's tensor for the two-dimensional Navier equation, given by

$$\mathbf{G}(\boldsymbol{x},\boldsymbol{y})=-\frac{1}{\mu}\Phi(\boldsymbol{x},\boldsymbol{y};\kappa_2)\mathbf{I}_2-\frac{1}{\omega^2}\nabla_{\boldsymbol{x}}\nabla_{\boldsymbol{x}}^{\top}\big(\Phi(\boldsymbol{x},\boldsymbol{y};\kappa_2)-\Phi(\boldsymbol{x},\boldsymbol{y};\kappa_1)\big),\tag{3.1}$$

where $\mathbf{I}_2$ is the 2×2 identity matrix and the scalar function

$$\Phi(\boldsymbol{x},\boldsymbol{y};\kappa)=\frac{\mathrm{i}}{4}H_0^{(1)}(\kappa|\boldsymbol{x}-\boldsymbol{y}|)\tag{3.2}$$

is the fundamental solution for the two-dimensional Helmholtz equation. Here, $H_0^{(1)}$ is the Hankel function of the first kind with order zero. Denote by $\mathbf{G}_{\mathrm{H}}(\boldsymbol{x},\boldsymbol{y})$, $y_2>0$, the Green's tensor to the unperturbed Dirichlet boundary value problem in a half-plane:

$$\mu\Delta\mathbf{G}_{\mathrm{H}}(\boldsymbol{x},\boldsymbol{y})+(\lambda+\mu)\nabla\nabla\cdot\mathbf{G}_{\mathrm{H}}(\boldsymbol{x},\boldsymbol{y})+\omega^2\mathbf{G}_{\mathrm{H}}(\boldsymbol{x},\boldsymbol{y})=-\delta(\boldsymbol{x}-\boldsymbol{y})\mathbf{I}_2\quad\text{in}\quad x_2>0,\quad \boldsymbol{x}\neq\boldsymbol{y},$$
$$\mathbf{G}_{\mathrm{H}}(\boldsymbol{x},\boldsymbol{y})=0\quad\text{on}\quad x_2=0.$$

Below, the expression of $\mathbf{G}_{\mathrm{H}}$ is presented; see e.g. [4,5].

LEMMA 3.1. *The Green's tensor* $\mathbf{G}_{\mathrm{H}}(\cdot,\boldsymbol{y})$, $(\boldsymbol{y}\in\Omega)$ *can be expressed as*

$$\mathbf{G}_{\mathrm{H}}(\boldsymbol{x},\boldsymbol{y})=\mathbf{G}(\boldsymbol{x},\boldsymbol{y})-\mathbf{G}(\boldsymbol{x},\boldsymbol{y}')+\mathbf{U}(\boldsymbol{x},\boldsymbol{y}),$$
$$\mathbf{U}(\boldsymbol{x},\boldsymbol{y})=-\frac{\mathrm{i}}{2\pi\omega^2}\int_{-\infty}^{\infty}\Big(\mathbf{M}_{\mathrm{p}}(\xi,\gamma_{\mathrm{p}},\gamma_{\mathrm{s}};x_2,y_2)+\mathbf{M}_{\mathrm{s}}(\xi,\gamma_{\mathrm{p}},\gamma_{\mathrm{s}};x_2,y_2)\Big)e^{-\mathrm{i}(x_1-y_1)\xi}\mathrm{d}\xi,\tag{3.3}$$

where

$$\mathbf{M}_{\mathrm{p}}(\xi,\gamma_{\mathrm{p}},\gamma_{\mathrm{s}};x_2,y_2)=\frac{e^{\mathrm{i}\gamma_{\mathrm{p}}(\mathrm{x}_2+\mathrm{y}_2)}-e^{\mathrm{i}(\gamma_{\mathrm{p}}\mathrm{x}_2+\gamma_{\mathrm{s}}\mathrm{y}_2)}}{\gamma_{\mathrm{p}}\gamma_{\mathrm{s}}+\xi^2}\begin{bmatrix}-\xi^2\gamma_{\mathrm{s}} & \xi^3\\ \xi\gamma_{\mathrm{p}}\gamma_{\mathrm{s}} & -\xi^2\gamma_{\mathrm{p}},\end{bmatrix}$$
$$\mathbf{M}_{\mathrm{s}}(\xi,\gamma_{\mathrm{p}},\gamma_{\mathrm{s}};x_2,y_2)=\frac{e^{\mathrm{i}\gamma_{\mathrm{s}}(\mathrm{x}_2+\mathrm{y}_2)}-e^{\mathrm{i}(\gamma_{\mathrm{s}}\mathrm{x}_2+\gamma_{\mathrm{p}}\mathrm{y}_2)}}{\gamma_{\mathrm{p}}\gamma_{\mathrm{s}}+\xi^2}\begin{bmatrix}-\xi^2\gamma_{\mathrm{s}} & -\xi\gamma_{\mathrm{p}}\gamma_{\mathrm{s}}\\ -\xi^3 & -\xi^2\gamma_{\mathrm{p}},\end{bmatrix}$$

Here, $\boldsymbol{y}'=(y_1,-y_2)$, *for* $\boldsymbol{y}=(y_1,y_2)\in\mathbb{R}^2$, $\gamma_{\mathrm{p}}=\sqrt{\kappa_1^2-\xi^2}$, $\gamma_{\mathrm{s}}=\sqrt{\kappa_2^2-\xi^2}$. *Moreover, the columns of the matrix function* $\mathbf{G}_{\mathrm{H}}(\cdot,\boldsymbol{y})$ *and the rows of the matrix function* $\mathbf{G}_{\mathrm{H}}(\boldsymbol{x},\cdot)$ *satisfy the half-plane Kupradze radiation condition.*

We introduce the generalized stress (or traction) operator on S_R, defined by

$$T_{a,b}u=(\mu+a)\partial_{\boldsymbol{\nu}}\boldsymbol{u}+b\boldsymbol{\nu}\nabla\cdot\boldsymbol{u}-a\boldsymbol{\tau}\mathrm{curl}\boldsymbol{u},\tag{3.4}$$

where $\boldsymbol{\nu}=(\nu_1,\nu_2)$ denotes the unit normal directed into the exterior of Ω_R, $\boldsymbol{\tau}:=(-\nu_2,\nu_1)$ is the tangential vector, and a and b are real numbers satisfying $a+b=\lambda+\mu$. Throughout this paper, we choose

$$a=\frac{\mu(\lambda+\mu)}{\lambda+3\mu},\quad b=\frac{(\lambda+\mu)(\lambda+2\mu)}{\lambda+3\mu}.$$

For simplicity, we denote $T_{a,b}$ by $T_{\boldsymbol{\nu}}$. With this choice, by Betti's formula, we obtain the following variational formulation: find $\boldsymbol{u}\in X_R$ such that

$$\int_{\Omega_R}\varepsilon(\boldsymbol{u},\overline{\boldsymbol{\varphi}})-\omega^2\boldsymbol{u}\cdot\overline{\boldsymbol{\varphi}}\mathrm{d}x-\int_{S_R}\overline{\boldsymbol{\varphi}}\cdot T_{\boldsymbol{\nu}}\boldsymbol{u}\mathrm{d}s=0 \tag{3.5}$$

for all $\boldsymbol{\varphi}\in X_R$, where

$$\begin{aligned}\varepsilon(\boldsymbol{u},\boldsymbol{\varphi})=&(2\mu+\lambda)(\partial_1u_1\partial_1\varphi_1+\partial_2u_2\partial_2\varphi_2)+\mu(\partial_2u_1\partial_2\varphi_1+\partial_1u_2\partial_1\varphi_2)\\&+\frac{(\lambda+\mu)(\lambda+2\mu)}{\lambda+3\mu}(\partial_1u_1\partial_2\varphi_2+\partial_2u_2\partial_1\varphi_1)+\frac{\mu(\lambda+\mu)}{\lambda+3\mu}(\partial_2u_1\partial_1\varphi_2+\partial_1u_2\partial_2\varphi_1).\end{aligned}$$

We note that the above symmetric sesquilinear form $\varepsilon(\cdot,\cdot)$ and the associated boundary operator $T_{\boldsymbol{\nu}}$ differ from the usual ones. In this case, $T_{\boldsymbol{\nu}}$ is called the pseudo stress operator [22]. We refer to [4,22] for a general form of the Betti's formula. The following lemma gives the coercive estimate of $\varepsilon(\cdot,\cdot)$.

LEMMA 3.2. *The symmetric sesquilinear form $\varepsilon(\cdot,\cdot)$ has the coercive estimate*

$$\int_{\Omega_R}\varepsilon(\boldsymbol{u},\bar{\boldsymbol{u}})\mathrm{d}\boldsymbol{x}\geq\frac{2\mu^2}{\lambda+3\mu}\int_{\Omega_R}|\nabla\boldsymbol{u}|^2\mathrm{d}\boldsymbol{x}. \tag{3.6}$$

Proof. From the definition of $\varepsilon(\cdot,\cdot)$, we have

$$\begin{aligned}\varepsilon(\boldsymbol{u},\bar{\boldsymbol{u}})=&(\lambda+2\mu)(|\partial_1u_1|^2+|\partial_2u_2|^2)+\mu(|\partial_2u_1|^2+|\partial_1u_2|^2)\\&+\frac{(\lambda+\mu)(\lambda+2\mu)}{\lambda+3\mu}(\partial_1u_1\partial_2\bar{u}_2+\partial_2u_2\partial_1\bar{u}_1)+\frac{\mu(\lambda+\mu)}{\lambda+3\mu}(\partial_2u_1\partial_1\bar{u}_2+\partial_1u_2\partial_2\bar{u}_1)\\=&(\lambda+2\mu)(|\partial_1u_1|^2+|\partial_2u_2|^2)+\mu(|\partial_2u_1|^2+|\partial_1u_2|^2)\\&+\frac{(\lambda+\mu)(\lambda+2\mu)}{\lambda+3\mu}2\mathrm{Re}(\partial_1u_1\partial_2\bar{u}_2)+\frac{\mu(\lambda+\mu)}{\lambda+3\mu}2\mathrm{Re}(\partial_2u_1\partial_1\bar{u}_2).\end{aligned}$$

By $\mu>0$ and $\lambda+\mu>0$, we have $\lambda+\mu>\frac{(\lambda+\mu)(\lambda+2\mu)}{\lambda+3\mu}$. On the other hand, we have

$$|2\mathrm{Re}(\partial_1u_1\partial_2\bar{u}_2)|\leq|\partial_1u_1|^2+|\partial_2u_2|^2.$$

Hence we can obtain that

$$\begin{aligned}&(\lambda+2\mu)(|\partial_1u_1|^2+|\partial_2u_2|^2)+\frac{(\lambda+\mu)(\lambda+2\mu)}{\lambda+3\mu}2\mathrm{Re}(\partial_1u_1\partial_2\bar{u}_2)\\\geq&\Big(\lambda+2\mu-\frac{(\lambda+\mu)(\lambda+2\mu)}{\lambda+3\mu}\Big)(|\partial_1u_1|^2+|\partial_2u_2|^2)\\=&\frac{2\mu(\lambda+2\mu)}{\lambda+3\mu}(|\partial_1u_1|^2+|\partial_2u_2|^2).\end{aligned} \tag{3.7}$$

Similarly, since $\mu > \frac{\mu(\lambda+\mu)}{\lambda+3\mu}$ and

$$|2\mathrm{Re}(\partial_2 u_1 \partial_1 \bar{u}_2)| \le |\partial_2 u_1|^2 + |\partial_1 u_2|^2,$$

we have

$$\begin{aligned}
&\mu(|\partial_2 u_1|^2 + |\partial_1 u_2|^2) + \frac{\mu(\lambda+\mu)}{\lambda+3\mu} 2\mathrm{Re}(\partial_2 u_1 \partial_1 \bar{u}_2) \\
\ge &\Big(\mu - \frac{\mu(\lambda+\mu)}{\lambda+3\mu}\Big)(|\partial_2 u_1|^2 + |\partial_1 u_2|^2) \\
= &\frac{2\mu^2}{\lambda+3\mu}(|\partial_2 u_1|^2 + |\partial_1 u_2|^2). \qquad (3.8)
\end{aligned}$$

Consequently, combining (3.7) and (3.8) and from $\frac{2\mu(\lambda+2\mu)}{\lambda+3\mu} > \frac{2\mu^2}{\lambda+3\mu}$, we have

$$\varepsilon(\boldsymbol{u}, \bar{\boldsymbol{u}}) \ge \frac{2\mu^2}{\lambda+3\mu}(|\partial_1 u_1|^2 + |\partial_2 u_2|^2 + |\partial_2 u_1|^2 + |\partial_1 u_2|^2),$$

which completes the proof. ∎

By applying Green's formula and the half-plane Kupradze radiation condition it is easy to derive the Green's representation formula for the scattered wave $\boldsymbol{u}^{\mathrm{sc}}$:

$$\boldsymbol{u}^{\mathrm{sc}} = \int_{S_R} T_{\boldsymbol{\nu}(\boldsymbol{y})} \mathbf{G}_{\mathrm{H}}(\boldsymbol{x}, \boldsymbol{y}) \cdot \boldsymbol{u}^{\mathrm{sc}}(\boldsymbol{y}) - \mathbf{G}_{\mathrm{H}}(\boldsymbol{x}, \boldsymbol{y}) \cdot T_{\boldsymbol{\nu}(\boldsymbol{y})} \boldsymbol{u}^{\mathrm{sc}}(\boldsymbol{y}) \mathrm{d}s(\boldsymbol{y}), \quad \boldsymbol{x} \in \Omega \backslash \overline{\Omega_R}. \qquad (3.9)$$

Taking the limit $\boldsymbol{x} \to S_R$ in (3.9) and setting $\boldsymbol{p} = T_{\boldsymbol{\nu}} \boldsymbol{u}^{\mathrm{sc}}|_{S_R} \in H^{-1/2}(S_R)^2$, we obtain

$$(\frac{1}{2}\mathcal{I} - \mathcal{D})(\boldsymbol{u}^{\mathrm{sc}}|_{S_R}) + \mathcal{S}\boldsymbol{p} = 0 \quad \text{on } S_R. \qquad (3.10)$$

Here $\mathcal{I}$ is the identity operator, $\mathcal{D}$ and $\mathcal{S}$ are the double layer and single layer operators over S_R, respectively, defined by

$$\begin{aligned}
(\mathcal{D}\boldsymbol{g})(\boldsymbol{x}) &= \int_{S_R} T_{\boldsymbol{\nu}(\boldsymbol{y})} \mathbf{G}_{\mathrm{H}}(\boldsymbol{x}, \boldsymbol{y}) \cdot \boldsymbol{g}(\boldsymbol{y}) \mathrm{d}s(\boldsymbol{y}), \\
(\mathcal{S}\boldsymbol{g})(\boldsymbol{x}) &= \int_{S_R} \mathbf{G}_{\mathrm{H}}(\boldsymbol{x}, \boldsymbol{y}) \cdot \boldsymbol{g}(\boldsymbol{y}) \mathrm{d}s(\boldsymbol{y}). \qquad (3.11)
\end{aligned}$$

Combining (3.5) and (3.10) yields the variational formulation for the unknown solution pair $(\boldsymbol{u}, \boldsymbol{p}) \in X_R \times H^{-1/2}(S_R)^2 := X$ as the following

$$\mathbb{B}((\boldsymbol{u}, \boldsymbol{p}), (\boldsymbol{\varphi}, \boldsymbol{\chi})) = \begin{bmatrix} b_1((\boldsymbol{u}, \boldsymbol{p}), (\boldsymbol{\varphi}, \boldsymbol{\chi})) \\ b_2((\boldsymbol{u}, \boldsymbol{p}), (\boldsymbol{\varphi}, \boldsymbol{\chi})) \end{bmatrix} = \begin{bmatrix} \int_{S_R} T_{\boldsymbol{\nu}} \boldsymbol{u}_0 \cdot \overline{\boldsymbol{\varphi}} \mathrm{d}s \\ \int_{S_R} (\frac{1}{2}\mathcal{I} - \mathcal{D})(\boldsymbol{u}_0|_{S_R}) \cdot \overline{\boldsymbol{\chi}} \mathrm{d}s \end{bmatrix} \qquad (3.12)$$

for all $(\boldsymbol{\varphi}, \boldsymbol{\chi}) \in X$, where $\boldsymbol{u}_0 = \boldsymbol{u}^{\mathrm{in}} + \boldsymbol{u}^{\mathrm{re}}$ is the reference field and

$$\begin{aligned}
b_1((\boldsymbol{u}, \boldsymbol{p}), (\boldsymbol{\varphi}, \boldsymbol{\chi})) &= \int_{\Omega_R} \varepsilon(\boldsymbol{u}, \overline{\boldsymbol{\varphi}}) - \omega^2 \boldsymbol{u} \cdot \overline{\boldsymbol{\varphi}} \mathrm{d}x - \int_{S_R} \overline{\boldsymbol{\varphi}} \cdot \boldsymbol{p} \mathrm{d}s, \\
b_2((\boldsymbol{u}, \boldsymbol{p}), (\boldsymbol{\varphi}, \boldsymbol{\chi})) &= \int_{S_R} \Big((\frac{1}{2}\mathcal{I} - \mathcal{D})(\boldsymbol{u}|_{S_R}) + \mathcal{S}\boldsymbol{p} \Big) \overline{\boldsymbol{\chi}} \mathrm{d}s.
\end{aligned}$$

REMARK 3.3. The variational formulation (3.12) and our scattering problem are equivalent in the following sense. If $u=u_0+u^{sc}$ is a solution to our original problem, then the restriction of u to Ω_R satisfies the variational Equation (3.12). On the other hand, if $u\in X_R$ is a solution to (3.12), then one may extend u^{sc} from Ω_R to $\Omega\backslash\overline{\Omega}_R$ through (3.9). It follows from (3.10) that the jump of u^{sc} is continuous at S_R, and if ω^2 is not a Dirichlet eigenvalue of the operator $-(\mu\Delta+(\lambda+\mu)\nabla(\nabla\cdot))$ over B_R^+, the jump of $\partial_\nu u^{sc}$ is also continuous at S_R. Hence, $u\in H^1_{loc}(\Omega)$ and $u-u_0$ satisfies the radiation solution (2.10). Note that we can always choose $R>0$ such that ω^2 is not the Dirichlet eigenvalue. This implies that the inverse of $\mathcal{S}$ exists.

Below we state the well-posedness of the direct scattering problem.

THEOREM 3.1. *For any incident plane wave at the frequency $\omega>0$, there exists a unique solution $\boldsymbol{u}\in X_R$ of the form $\boldsymbol{u}=\boldsymbol{u}^{\text{in}}+\boldsymbol{u}^{\text{re}}+\boldsymbol{u}^{sc}$ where the scattered field $\boldsymbol{u}^{sc}$ satisfies the half-plane Kupradze radiation condition and the reference field $\boldsymbol{u}_0=\boldsymbol{u}^{\text{in}}+\boldsymbol{u}^{\text{re}}$ is given by (2.6).*

Proof. Since Γ_f is the graph of a Lipschitz function, from solvability of rough surface scattering [14], there exists a unique solution $\boldsymbol{v}:=\boldsymbol{u}-\boldsymbol{u}^{\text{in}}$ which fulfills the Upward Propagation Radiation Condition (UPRC) for the Navier equation. Since the UPRC covers outgoing plane waves and the Sommerfeld radiation solutions, we get $\boldsymbol{u}^{\text{sc}}=\boldsymbol{u}^{re}=0$ if $\boldsymbol{u}^{\text{in}}=0$. This proves uniqueness. To prove the existence of $\boldsymbol{u}^{\text{sc}}$, we only need to show that the variational formulation (3.12) is of Fredholm type.

By Riesz representation theorem, there exist linear operators

$$\begin{aligned}
T_1, J_1 &: H^1_{\Lambda_R}(\Omega)^2 \to H^{-1}_{\Lambda_R}(\Omega)^2,\\
T_2 &: H^{-1/2}(S_R)^2 \to H^{-1}_{\Lambda_R}(\Omega)^2,\\
T_3 &: H^{-1/2}(S_R)^2 \to \tilde{H}^{1/2}(S_R)^2,\\
J_2 &: H^1_{\Lambda_R}(\Omega_R)^2 \to \tilde{H}^{1/2}(S_R)^2,
\end{aligned}$$

such that for $(\boldsymbol{u},\boldsymbol{p}),(\boldsymbol{\varphi},\boldsymbol{\chi})\in X$,

$$\begin{aligned}
(T_1\boldsymbol{u},\boldsymbol{\varphi}) &:= \frac{1}{2}\int_{\Omega_R} \boldsymbol{\varepsilon}(\boldsymbol{u},\bar{\boldsymbol{\varphi}})+\omega^2\boldsymbol{u}\cdot\bar{\boldsymbol{\varphi}}\,\mathrm{d}\boldsymbol{x},\\
(J_1\boldsymbol{u},\boldsymbol{\varphi}) &:= -\int_{\Omega_R} \omega^2\boldsymbol{u}\cdot\bar{\boldsymbol{\varphi}}\,\mathrm{d}\boldsymbol{x},\\
\langle T_2\boldsymbol{p},\boldsymbol{\varphi}\rangle &:= \frac{1}{2}\int_{S_R} \boldsymbol{p}\cdot\bar{\boldsymbol{\varphi}}\,\mathrm{d}s,\\
\langle T_3\boldsymbol{p},\boldsymbol{\chi}\rangle &:= \int_{S_R} \mathcal{S}\boldsymbol{p}\cdot\bar{\boldsymbol{\chi}}\,\mathrm{d}s,\\
\langle J_2\boldsymbol{u},\boldsymbol{\chi}\rangle &:= -\int_{S_R} \mathcal{D}(\boldsymbol{u}|_{S_R})\cdot\bar{\boldsymbol{\chi}}\,\mathrm{d}s.
\end{aligned}$$

Here $(\cdot,\cdot)$ denotes the duality between $H^1_{\Lambda_R}(\Omega_R)^2$ and $H^{-1}_{\Lambda_R}(\Omega_R)^2$, whereas $\langle\cdot,\cdot\rangle$ the duality between $\tilde{H}^{1/2}(S_R)^2$ and $H^{-1/2}(S_R)^2$. By Sobolev embedding theorems, J_1 is compact. The operator J_2 is also compact, since the double layer operator $\mathcal{D}:\tilde{H}^{1/2}(S_R)^2\to\tilde{H}^{1/2}(S_R)^2$ is compact (see [29]). This follows from the special choice of the values a and b in the definition of the generalized stress operator, for which the kernel in the definition of the double layer operator $\mathcal{D}$ has a weak singularity (see Chapter 3 in [3]).

Then, we may rewrite $\mathbb{B}: X \times X \to \mathbb{C}^2$ as

$$\mathbb{B}((\boldsymbol{u},\boldsymbol{p}),(\boldsymbol{\varphi},\boldsymbol{\chi})) = \langle \mathbb{B}_1(\boldsymbol{u},\boldsymbol{p}),(\boldsymbol{\varphi},\boldsymbol{\chi})\rangle + \langle \mathbb{B}_2(\boldsymbol{u},\boldsymbol{p}),(\boldsymbol{\varphi},\boldsymbol{\chi})\rangle$$

where $\langle\cdot,\cdot\rangle$ denotes the duality between X and X^{-1}, and the operators $\mathbb{B}_j: X \to X^{-1}$, $j = 1,2$ are defined as

$$\mathbb{B}_1 := \begin{bmatrix} T_1 & -T_2 \\ T_2^* & T_3 \end{bmatrix}, \quad \mathbb{B}_2 := \begin{bmatrix} J_1 & 0 \\ J_2 & 0 \end{bmatrix}.$$

By Lemma 3.2, T_1 is a coercive operator over $H^1_{\Lambda_R}(\Omega_R)^2$. Following the arguments in the proof of [29, Theorem 7.6], one can prove that T_3 is a strongly elliptic operator over $H^{-1/2}(S_R)^2$. Hence, the real part of $\mathbb{B}_1$, given by

$$\mathrm{Re}\mathbb{B}_1 := \frac{\mathbb{B}_1 + \mathbb{B}_1^*}{2} = \begin{bmatrix} T_1 & \\ & T_3 \end{bmatrix}$$

is strongly elliptic over X. Since $\mathbb{B}_2$ is also compact, the operator $\mathbb{B}$ is Fredholm with index zero. Applying the Fredholm alternative yields the existence of solutions. ∎

REMARK 3.4. Once the data of $\boldsymbol{u}^{sc}$ are computed on $\overline{\Omega}_R$, the far-field pattern of $\boldsymbol{u}^{sc}$ can be represented as

$$\boldsymbol{u}^{\infty}(\hat{\boldsymbol{x}}) = \int_{S_R} \boldsymbol{G}_H^{\infty}(\hat{\boldsymbol{x}},\boldsymbol{y}) \cdot T_{\nu(\boldsymbol{y})}[u^{sc}(\boldsymbol{y})] - T_{\nu(\boldsymbol{y})}[\boldsymbol{G}_H^{\infty}(\hat{\boldsymbol{x}},\boldsymbol{y})] \cdot u^{sc}(\boldsymbol{y})\, \mathrm{d}s(\boldsymbol{y}), \tag{3.13}$$

where $G_H^{\infty}(\hat{\boldsymbol{x}},\boldsymbol{y})$ stands for the far-field pattern of the function $\boldsymbol{x} \to \boldsymbol{G}_H^{\infty}(\boldsymbol{x},\boldsymbol{y})$ as $|\boldsymbol{x}| \to \infty$ in the upper half-space.

4. Inverse scattering

In this section, we study the domain derivative and propose a continuation method for the inverse scattering problem. Throughout this section, we suppose that ω^2 is not a Dirichlet eigenvalue of the Navier equation in B_R^+. Note that this assumption can always be fulfilled by slightly changing R. For simplicity, in this section, we define the traction operator by (that is, we take $a = 0$, $b = \lambda + \mu$ in (3.4))

$$T_{\boldsymbol{\nu}}\boldsymbol{u} := \mu \partial_{\boldsymbol{\nu}} \boldsymbol{u} + (\lambda + \mu)(\nabla \cdot \boldsymbol{u})\boldsymbol{\nu} \quad \text{on } S_R.$$

Then the symmetric sesquilinear form $\varepsilon(\cdot,\cdot)$ can be rewritten as

$$\varepsilon(\boldsymbol{u},\boldsymbol{\varphi}) = \mu \nabla \boldsymbol{u} : \nabla \boldsymbol{\varphi} + (\lambda + \mu)(\nabla \cdot \boldsymbol{u})(\nabla \cdot \boldsymbol{\varphi}).$$

Here $A : B = \mathrm{tr}(AB^{\top})$ is the Frobenius inner product of square matrices A and B.

4.1. Domain derivative. Given $h > 0$, introduce a domain Ω_R^h bounded by Λ_R^h and S_R, where

$$\Lambda_R^h = \{\boldsymbol{x} + h\boldsymbol{p}(\boldsymbol{x}) : \boldsymbol{x} \in \Lambda_R\},$$

Here, the profile function f is assumed to be in $C^2(\mathbb{R})$ and the function $\boldsymbol{p} = (p_1(\boldsymbol{x}), p_2(\boldsymbol{x}))^{\top} \in C^2(\Lambda_R, \mathbb{R}^2)$ satisfies $\boldsymbol{p} = 0$ on boundary of the locally perturbed surface Λ_R. Since ω^2 is not an eigenvalue, the single layer operator defined in (3.11) is invertible. Hence, we introduce a Dirichlet-to-Neumann map on S_R:

$$T_{\boldsymbol{\nu}}\boldsymbol{u} = \mathcal{A}\boldsymbol{u} + \boldsymbol{g},$$

where

$$\mathcal{A} := -\mathcal{S}^{-1}(\frac{1}{2}\mathcal{I} - \mathcal{D}),$$

and

$$\boldsymbol{g} = T_{\boldsymbol{\nu}}\boldsymbol{u}_0 - \mathcal{A}\boldsymbol{u}_0.$$

Consider the variational problem in the perturbed domain Ω_R^h: Find $\boldsymbol{u}_h \in H^1_{\Lambda_R^h}(\Omega_R^h)^2$ such that

$$b^h(\boldsymbol{u}_h, \boldsymbol{v}_h) = \langle \boldsymbol{g}, \boldsymbol{v}_h \rangle_{S_R}, \quad \forall \boldsymbol{v}_h \in H^1_{\Lambda_R}(\Omega_R^h)^2, \tag{4.1}$$

where the sesquilinear form $b^h : H^1_{\Lambda_R^h}(\Omega_R^h)^2 \times H^1_{\Lambda_R^h}(\Omega_R^h)^2 \to \mathbb{C}$ is defined by

$$\begin{aligned} b^h(\boldsymbol{u}_h, \boldsymbol{v}_h) = &\mu \int_{\Omega_R^h} \nabla \boldsymbol{u}_h : \nabla \bar{\boldsymbol{v}}_h \, \mathrm{d}\boldsymbol{y} + (\lambda + \mu) \int_{\Omega_R^h} (\nabla \cdot \boldsymbol{u}_h)(\nabla \cdot \bar{\boldsymbol{v}}_h) \, \mathrm{d}\boldsymbol{y} \\ &- \omega^2 \int_{\Omega_R^h} \boldsymbol{u}_h \cdot \bar{\boldsymbol{v}}_h \, \mathrm{d}\boldsymbol{y} - \langle \mathcal{A}\boldsymbol{u}_h, \boldsymbol{v}_h \rangle_{S_R}. \end{aligned} \tag{4.2}$$

Define a nonlinear scattering operator: $\mathcal{F}$

$$\mathcal{F} : \Lambda_R^h \to \gamma \boldsymbol{u}_h$$

where γ is the trace operator onto S_R. The domain derivative of the operator $\mathcal{F}$ on the boundary Λ_R along with the direction $\boldsymbol{p}$ is defined by

$$\mathcal{F}'(\Lambda_R; \boldsymbol{p}) := \lim_{h \to 0} \frac{\mathcal{F}(\Lambda_R^h) - \mathcal{F}(\Lambda_R)}{h} = \lim_{h \to 0} \frac{\gamma \boldsymbol{u}_h - \gamma \boldsymbol{u}}{h}.$$

For a given $\boldsymbol{p}$, we extend its domain to $\bar{\Omega}_R^+$ by requiring that $\boldsymbol{p}(\boldsymbol{x}) = (0,0)^\top$ if $|\boldsymbol{x}| > R - \alpha$ for some small positive constant α, and $\boldsymbol{y} = \xi^h(\boldsymbol{x}) = \boldsymbol{x} + h\boldsymbol{p}(\boldsymbol{x})$ maps Ω_R to Ω_R^h. It is clear to note that ξ^h is a diffeomorphism from Ω_R to Ω_R^h for sufficiently small h. Denote by $\eta^h(\boldsymbol{y}) : \Omega_R^h \to \Omega_R$ the inverse map of ξ^h.

Define $\breve{\boldsymbol{u}}(\boldsymbol{x}) = (\breve{u}_1, \breve{u}_2)^\top := (\boldsymbol{u}_h \circ \xi^h)(\boldsymbol{x})$. It follows from the change of variable $\boldsymbol{y} = \xi^h(\boldsymbol{x})$ that

$$\begin{aligned} \int_{\Omega_R^h} (\nabla \boldsymbol{u}_h : \nabla \bar{\boldsymbol{v}}_h) \, \mathrm{d}\boldsymbol{y} &= \sum_{j=1}^{2} \int_{\Omega_R} \nabla \breve{u}_j J_{\eta^h} J_{\eta^h}^\top \nabla \bar{\breve{v}}_j \det(J_{\xi^h}) \, \mathrm{d}\boldsymbol{x}, \\ \int_{\Omega_R^h} (\nabla \cdot \boldsymbol{u}_h)(\nabla \cdot \bar{\boldsymbol{v}}_h) \, \mathrm{d}\boldsymbol{y} &= \int_{\Omega_R} (\nabla \breve{\boldsymbol{u}} : J_{\eta^h}^\top)(\nabla \bar{\breve{\boldsymbol{v}}} : J_{\eta^h}^\top) \det(J_{\xi^h}) \, \mathrm{d}\boldsymbol{x}, \\ \int_{\Omega_R^h} \boldsymbol{u}_h \cdot \bar{\boldsymbol{v}}_h \, \mathrm{d}\boldsymbol{y} &= \int_{\Omega_R} \breve{\boldsymbol{u}} \cdot \bar{\breve{\boldsymbol{v}}} \det(J_{\xi^h}) \, \mathrm{d}\boldsymbol{x}, \end{aligned}$$

where $\breve{\boldsymbol{v}}(\boldsymbol{x}) = (\breve{v}_1, \breve{v}_2)^\top := (\boldsymbol{v}_h \circ \xi^h)(\boldsymbol{x})$, J_{η^h} and J_{ξ^h} are the Jacobian matrices of the transforms η^h and ξ^h, respectively.

For an arbitrary test function $\boldsymbol{v}_h$ in the domain Ω_R^h, it is easy to note that $\breve{\boldsymbol{v}}$ is a test function in the domain Ω_R, according to the transform. Therefore, the sesquilinear form b^h in (4.2) becomes

$$b^h(\breve{\boldsymbol{u}}, \boldsymbol{v}) = \sum_{j=1}^{2} \mu \int_{\Omega_R} \nabla \breve{u}_j J_{\eta^h} J_{\eta^h}^\top \nabla \bar{v}_j \det(J_{\xi^h}) \, \mathrm{d}\boldsymbol{x} + (\lambda + \mu) \int_{\Omega_R} (\nabla \breve{\boldsymbol{u}} : J_{\eta^h}^\top)$$

$$\times(\nabla\bar{\boldsymbol{v}}:J_{\eta^h}^{\top})\det(J_{\xi^h})\,\mathrm{d}\boldsymbol{x}-\omega^2\int_{\Omega_R}\breve{\boldsymbol{u}}\cdot\bar{\boldsymbol{v}}\det(J_{\xi^h})\,\mathrm{d}\boldsymbol{x}-\langle\mathcal{A}\breve{\boldsymbol{u}},\boldsymbol{v}\rangle_{\partial B_R^+},$$

which gives an equivalent variational formulation to (4.1):

$$b^h(\breve{\boldsymbol{u}},\boldsymbol{v})=\langle\boldsymbol{g},\boldsymbol{v}\rangle_{\partial B_R^+},\quad\forall\boldsymbol{v}\in H^1_{\Lambda_R}(\Omega_R)^2. \tag{4.3}$$

A simple calculation yields

$$b(\breve{\boldsymbol{u}}-\boldsymbol{u},\boldsymbol{v})=b(\breve{\boldsymbol{u}},\boldsymbol{v})-\langle\boldsymbol{g},\boldsymbol{v}\rangle_{\partial B_R^+}=b(\breve{\boldsymbol{u}},\boldsymbol{v})-b^h(\breve{\boldsymbol{u}},\boldsymbol{v})=b_1+b_2+b_3,$$

where

$$b_1=\sum_{j=1}^{2}\mu\int_{\Omega_R}\nabla\breve{u}_j\left(I-J_{\eta^h}J_{\eta^h}^{\top}\det(J_{\xi^h})\right)\nabla\bar{v}_j\,\mathrm{d}\boldsymbol{x}, \tag{4.4}$$

$$b_2=(\lambda+\mu)\int_{\Omega_R}(\nabla\cdot\breve{\boldsymbol{u}})(\nabla\cdot\bar{\boldsymbol{v}})-(\nabla\breve{\boldsymbol{u}}:J_{\eta^h}^{\top})(\nabla\bar{\boldsymbol{v}}:J_{\eta^h}^{\top})\det(J_{\xi^h})\,\mathrm{d}\boldsymbol{x}, \tag{4.5}$$

$$b_3=\omega^2\int_{\Omega_R}\breve{\boldsymbol{u}}\cdot\bar{\boldsymbol{v}}\left(\det(J_{\xi^h})-1\right)\mathrm{d}\boldsymbol{x}. \tag{4.6}$$

Here I is the identity matrix. Following the definitions of the Jacobian matrices, we may easily verify that

$$\begin{aligned}\det(J_{\xi^h})&=1+h\nabla\cdot\boldsymbol{p}+O(h^2),\\ J_{\eta^h}&=J_{\xi^h}^{-1}\circ\eta^h=I-hJ_{\boldsymbol{p}}+O(h^2),\\ J_{\eta^h}J_{\eta^h}^{\top}\det(J_{\xi^h})&=I-h(J_{\boldsymbol{p}}+J_{\boldsymbol{p}}^{\top})+h(\nabla\cdot\boldsymbol{p})I+O(h^2),\end{aligned}$$

where the matrix $J_{\boldsymbol{p}}=\nabla\boldsymbol{p}$. Substituting the above estimates into (4.4)-(4.6), we obtain

$$\begin{aligned}b_1&=\sum_{j=1}^{2}\mu\int_{\Omega_R}\nabla\breve{u}_j\left(h(J_{\boldsymbol{p}}+J_{\boldsymbol{p}}^{\top})-h(\nabla\cdot\boldsymbol{p})I+O(h^2)\right)\nabla\bar{v}_j\,\mathrm{d}\boldsymbol{x},\\ b_2&=(\lambda+\mu)\int_{\Omega_R}h(\nabla\cdot\breve{\boldsymbol{u}})(\nabla\bar{\boldsymbol{v}}:J_{\boldsymbol{p}}^{\top})+h(\nabla\cdot\bar{\boldsymbol{v}})(\nabla\breve{\boldsymbol{u}}:J_{\boldsymbol{p}}^{\top})\\ &\quad-h(\nabla\cdot\boldsymbol{p})(\nabla\cdot\breve{\boldsymbol{u}})(\nabla\cdot\bar{\boldsymbol{v}})+O(h^2)\,\mathrm{d}\boldsymbol{x},\\ b_3&=\omega^2\int_{\Omega_R}\breve{\boldsymbol{u}}\cdot\bar{\boldsymbol{v}}\left(h\nabla\cdot\boldsymbol{p}+O(h^2)\right)\mathrm{d}\boldsymbol{x}.\end{aligned}$$

Hence we have

$$b\left(\frac{\breve{\boldsymbol{u}}-\boldsymbol{u}}{h},\boldsymbol{v}\right)=g_1(\boldsymbol{p})(\breve{\boldsymbol{u}},\boldsymbol{v})+g_2(\boldsymbol{p})(\breve{\boldsymbol{u}},\boldsymbol{v})+g_3(\boldsymbol{p})(\breve{\boldsymbol{u}},\boldsymbol{v})+O(h), \tag{4.7}$$

where

$$\begin{aligned}g_1&=\sum_{j=1}^{2}\mu\int_{\Omega_R}\nabla\breve{u}_j\left((J_{\boldsymbol{p}}+J_{\boldsymbol{p}}^{\top})-(\nabla\cdot\boldsymbol{p})I\right)\nabla\bar{v}_j\,\mathrm{d}\boldsymbol{x},\\ g_2&=(\lambda+\mu)\int_{\Omega_R}(\nabla\cdot\breve{\boldsymbol{u}})(\nabla\bar{\boldsymbol{v}}:J_{\boldsymbol{p}}^{\top})+(\nabla\cdot\bar{\boldsymbol{v}})(\nabla\breve{\boldsymbol{u}}:J_{\boldsymbol{p}}^{\top})-(\nabla\cdot\boldsymbol{p})(\nabla\cdot\breve{\boldsymbol{u}})(\nabla\cdot\bar{\boldsymbol{v}})\,\mathrm{d}\boldsymbol{x},\end{aligned}$$

$$g_3 = \omega^2 \int_{\Omega_R} (\nabla \cdot \boldsymbol{p}) \breve{\boldsymbol{u}} \cdot \bar{\boldsymbol{v}} \, \mathrm{d}\boldsymbol{x}.$$

THEOREM 4.1. *Let $\boldsymbol{u}$ be the solution of problem (2.4). Given $\boldsymbol{p}$, the domain derivative of the scattering operator $\mathcal{F}$ is $\mathcal{F}'(\Lambda_R;\boldsymbol{p}) = \gamma \boldsymbol{u}'$, where $\boldsymbol{u}'$ is the unique weak solution of the boundary value problem:*

$$\begin{cases} \mu \Delta \boldsymbol{u}' + (\lambda+\mu) \nabla \nabla \cdot \boldsymbol{u}' + \omega^2 \boldsymbol{u}' = 0 & \text{in } \Omega_R, \\ \boldsymbol{u}' = -(\boldsymbol{p} \cdot \boldsymbol{\nu}) \partial_{\boldsymbol{\nu}} \boldsymbol{u} & \text{on } \Lambda_R, \\ \mu \partial_{\boldsymbol{\nu}} \boldsymbol{u}' + (\lambda+\mu)(\nabla \cdot \boldsymbol{u}') \boldsymbol{\nu} = \mathcal{A} \boldsymbol{u}' & \text{on } S_R. \end{cases} \tag{4.8}$$

Proof. Given $\boldsymbol{p}$, we extend it to $\bar{\Omega}_R^+$ as before. It follows from the well-posedness of problem (3.12) that $\breve{\boldsymbol{u}} \to \boldsymbol{u}$ in $H^1_{\Lambda_R}(\Omega_R)^2$ as $h \to 0$. Taking the limit $h \to 0$ in (4.7) gives

$$b\left(\lim_{h\to 0} \frac{\breve{\boldsymbol{u}} - \boldsymbol{u}}{h}, \boldsymbol{v} \right) = g_1(\boldsymbol{p})(\boldsymbol{u},\boldsymbol{v}) + g_2(\boldsymbol{p})(\boldsymbol{u},\boldsymbol{v}) + g_3(\boldsymbol{p})(\boldsymbol{u},\boldsymbol{v}), \tag{4.9}$$

which shows that $(\breve{\boldsymbol{u}} - \boldsymbol{u})/h$ is convergent in $H^1_{\Lambda_R}(\Omega_R)^2$ as $h \to 0$. Denote by $\dot{\boldsymbol{u}}$ this limit and rewrite (4.9) as

$$b(\dot{\boldsymbol{u}}, \boldsymbol{v}) = g_1(\boldsymbol{p})(\boldsymbol{u},\boldsymbol{v}) + g_2(\boldsymbol{p})(\boldsymbol{u},\boldsymbol{v}) + g_3(\boldsymbol{p})(\boldsymbol{u},\boldsymbol{v}). \tag{4.10}$$

First we compute $g_1(\boldsymbol{p})(\boldsymbol{u},\boldsymbol{v})$. Noting $\boldsymbol{p} = 0$ on S_R and using the identity

$$\begin{aligned} \nabla u \left((J_{\boldsymbol{p}} + J_{\boldsymbol{p}}^\top) - (\nabla \cdot \boldsymbol{p}) I \right) \nabla \bar{v} = {} & \nabla \cdot [(\boldsymbol{p} \cdot \nabla u) \nabla \bar{v} + (\boldsymbol{p} \cdot \nabla \bar{v}) \nabla u - (\nabla u \cdot \nabla \bar{v}) \boldsymbol{p}] \\ & - (\boldsymbol{p} \cdot \nabla u) \Delta \bar{v} - (\boldsymbol{p} \cdot \nabla \bar{v}) \Delta u, \end{aligned}$$

we obtain, from the divergence theorem, that

$$\begin{aligned} g_1(\boldsymbol{p})(\boldsymbol{u},\boldsymbol{v}) = {} & -\sum_{j=1}^2 \mu \int_{\Omega_R} (\boldsymbol{p} \cdot \nabla u_j) \Delta \bar{v}_j + (\boldsymbol{p} \cdot \nabla \bar{v}_j) \Delta u_j \, \mathrm{d}\boldsymbol{x} \\ & - \sum_{j=1}^2 \mu \int_{\Lambda_R} (\boldsymbol{p} \cdot \nabla u_j)(\boldsymbol{\nu} \cdot \nabla \bar{v}_j) + (\boldsymbol{p} \cdot \nabla \bar{v}_j)(\boldsymbol{\nu} \cdot \nabla u_j) - (\boldsymbol{p} \cdot \boldsymbol{\nu})(\nabla u_j \cdot \nabla \bar{v}_j) \, \mathrm{d}s \\ = {} & -\mu \int_{\Omega_R} (\boldsymbol{p} \cdot \nabla \boldsymbol{u}) \cdot \Delta \bar{\boldsymbol{v}} + (\boldsymbol{p} \cdot \nabla \bar{\boldsymbol{v}}) \cdot \Delta \boldsymbol{u} \, \mathrm{d}\boldsymbol{x} \\ & - \mu \int_{\Lambda_R} (\boldsymbol{p} \cdot \nabla \boldsymbol{u}) \cdot (\boldsymbol{\nu} \cdot \nabla \bar{\boldsymbol{v}}) + (\boldsymbol{p} \cdot \nabla \bar{\boldsymbol{v}}) \cdot (\boldsymbol{\nu} \cdot \nabla \boldsymbol{u}) - (\boldsymbol{p} \cdot \boldsymbol{\nu})(\nabla \boldsymbol{u} : \nabla \bar{\boldsymbol{v}}) \, \mathrm{d}s. \end{aligned}$$

Since $\mu \Delta \boldsymbol{u} + (\lambda+\mu) \nabla \nabla \cdot \boldsymbol{u} + \omega^2 \boldsymbol{u} = 0$ in Ω_R, we have, from the integration by parts, that

$$\begin{aligned} & \mu \int_{\Omega_R} (\boldsymbol{p} \cdot \nabla \bar{\boldsymbol{v}}) \cdot \Delta \boldsymbol{u} \, \mathrm{d}\boldsymbol{x} \\ = {} & -(\lambda+\mu) \int_{\Omega_R} (\boldsymbol{p} \cdot \nabla \bar{\boldsymbol{v}}) \cdot (\nabla \nabla \cdot \boldsymbol{u}) \, \mathrm{d}\boldsymbol{x} - \omega^2 \int_{\Omega_R} (\boldsymbol{p} \cdot \nabla \bar{\boldsymbol{v}}) \cdot \boldsymbol{u} \, \mathrm{d}\boldsymbol{x} \\ = {} & (\lambda+\mu) \int_{\Omega_R} (\nabla \cdot \boldsymbol{u}) \nabla \cdot (\boldsymbol{p} \cdot \nabla \bar{\boldsymbol{v}}) \, \mathrm{d}\boldsymbol{x} + (\lambda+\mu) \int_{\Lambda_R} (\nabla \cdot \boldsymbol{u})(\boldsymbol{\nu} \cdot (\boldsymbol{p} \cdot \nabla \bar{\boldsymbol{v}})) \, \mathrm{d}s \\ & - \omega^2 \int_{\Omega_R} (\boldsymbol{p} \cdot \nabla \bar{\boldsymbol{v}}) \cdot \boldsymbol{u} \, \mathrm{d}\boldsymbol{x}. \end{aligned}$$

Using the integration by parts again yields

$$\mu\int_{\Omega_R}(\boldsymbol{p}\cdot\nabla\boldsymbol{u})\cdot\Delta\bar{\boldsymbol{v}}\,\mathrm{d}\boldsymbol{x}=-\mu\int_{\Omega_R}\nabla(\boldsymbol{p}\cdot\nabla\boldsymbol{u}):\nabla\bar{\boldsymbol{v}}\,\mathrm{d}\boldsymbol{x}-\mu\int_{\Lambda_R}(\boldsymbol{p}\cdot\nabla\boldsymbol{u})\cdot(\boldsymbol{\nu}\cdot\nabla\bar{\boldsymbol{v}})\,\mathrm{d}s.$$

It is easy to verify that

$$\int_{\Lambda_R}(\boldsymbol{p}\cdot\nabla\bar{\boldsymbol{v}})\cdot(\boldsymbol{\nu}\cdot\nabla\boldsymbol{u})-(\boldsymbol{p}\cdot\boldsymbol{\nu})(\nabla\boldsymbol{u}:\nabla\bar{\boldsymbol{v}})\,\mathrm{d}s=0.$$

Noting $\boldsymbol{v}=0$ on Λ_R and

$$(\nabla\cdot\boldsymbol{p})(\boldsymbol{u}\cdot\bar{\boldsymbol{v}})+(\boldsymbol{p}\cdot\nabla\bar{\boldsymbol{v}})\cdot\boldsymbol{u}=\nabla\cdot((\boldsymbol{u}\cdot\bar{\boldsymbol{v}})\boldsymbol{p})-(\boldsymbol{p}\cdot\nabla\boldsymbol{u})\cdot\bar{\boldsymbol{v}},$$

we obtain by the divergence theorem that

$$\int_{\Omega_R}(\nabla\cdot\boldsymbol{p})(\boldsymbol{u}\cdot\bar{\boldsymbol{v}})+(\boldsymbol{p}\cdot\nabla\bar{\boldsymbol{v}})\cdot\boldsymbol{u}\,\mathrm{d}\boldsymbol{x}=-\int_{\Omega_R}(\boldsymbol{p}\cdot\nabla\boldsymbol{u})\cdot\bar{\boldsymbol{v}}\,\mathrm{d}\boldsymbol{x}.$$

Combining the above identities, we conclude that

$$\begin{aligned}g_1(\boldsymbol{p})(\boldsymbol{u},\boldsymbol{v})+g_3(\boldsymbol{p})(\boldsymbol{u},\boldsymbol{v})=\mu\int_{\Omega_R}\nabla(\boldsymbol{p}\cdot\nabla\boldsymbol{u}):\nabla\bar{\boldsymbol{v}}\,\mathrm{d}\boldsymbol{x}-(\lambda+\mu)\int_{\Omega_R}(\nabla\cdot\boldsymbol{u})\nabla\cdot(\boldsymbol{p}\cdot\nabla\bar{\boldsymbol{v}})\,\mathrm{d}\boldsymbol{x}\\-\omega^2\int_{\Omega_R}(\boldsymbol{p}\cdot\nabla\boldsymbol{u})\cdot\bar{\boldsymbol{v}}\,\mathrm{d}\boldsymbol{x}+(\lambda+\mu)\int_{\Lambda_R}(\nabla\cdot\boldsymbol{u})(\boldsymbol{\nu}\cdot(\boldsymbol{p}\cdot\nabla\bar{\boldsymbol{v}}))\,\mathrm{d}s.\end{aligned}\tag{4.11}$$

Next, we compute $g_2(\boldsymbol{p})(\boldsymbol{u},\boldsymbol{v})$. It is easy to verify that

$$\begin{aligned}\int_{\Omega_R}(\nabla\cdot\boldsymbol{u})(\nabla\bar{\boldsymbol{v}}:J_{\boldsymbol{p}}^{\top})+(\nabla\cdot\bar{\boldsymbol{v}})(\nabla\boldsymbol{u}:J_{\boldsymbol{p}}^{\top})\,\mathrm{d}\boldsymbol{x}&=\int_{\Omega_R}(\nabla\cdot\boldsymbol{u})\nabla\cdot(\boldsymbol{p}\cdot\nabla\bar{\boldsymbol{v}})\,\mathrm{d}\boldsymbol{x}\\&-\int_{\Omega_R}(\nabla\cdot\boldsymbol{u})(\boldsymbol{p}\cdot(\nabla\cdot(\nabla\boldsymbol{v})^{\top}))\,\mathrm{d}\boldsymbol{x}+\int_{\Omega_R}(\nabla\cdot\bar{\boldsymbol{v}})\nabla\cdot(\boldsymbol{p}\cdot\nabla\boldsymbol{u})\,\mathrm{d}\boldsymbol{x}\\&-\int_{\Omega_R}(\nabla\cdot\bar{\boldsymbol{v}})(\boldsymbol{p}\cdot(\nabla\cdot(\nabla\boldsymbol{u})^{\top}))\,\mathrm{d}\boldsymbol{x}.\end{aligned}$$

Using the integration by parts, we obtain

$$\begin{aligned}&\int_{\Omega_R}(\nabla\cdot\boldsymbol{p})(\nabla\cdot\boldsymbol{u})(\nabla\cdot\bar{\boldsymbol{v}})\,\mathrm{d}\boldsymbol{x}\\&=-\int_{\Omega_R}\boldsymbol{p}\cdot\nabla((\nabla\cdot\boldsymbol{u})(\nabla\cdot\bar{\boldsymbol{v}}))\,\mathrm{d}\boldsymbol{x}-\int_{\Lambda_R}(\nabla\cdot\boldsymbol{u})(\nabla\cdot\bar{\boldsymbol{v}})(\boldsymbol{\nu}\cdot\boldsymbol{p})\,\mathrm{d}s\\&=-\int_{\Omega_R}(\nabla\cdot\bar{\boldsymbol{v}})(\boldsymbol{p}\cdot(\nabla\cdot(\nabla\boldsymbol{u})^{\top}))\,\mathrm{d}\boldsymbol{x}-\int_{\Omega_R}(\nabla\cdot\boldsymbol{u})(\boldsymbol{p}\cdot(\nabla\cdot(\nabla\boldsymbol{v})^{\top}))\,\mathrm{d}\boldsymbol{x}\\&\quad-\int_{\Lambda_R}(\nabla\cdot\boldsymbol{u})(\nabla\cdot\bar{\boldsymbol{v}})(\boldsymbol{\nu}\cdot\boldsymbol{p})\,\mathrm{d}s.\end{aligned}$$

Since $\boldsymbol{v}=0$ on Λ_R, we have $\partial_{\boldsymbol{\tau}}\boldsymbol{v}=0$, which implies that

$$\nu_2\partial_{x_1}v_1=\nu_1\partial_{x_2}v_1,\quad \nu_2\partial_{x_1}v_2=\nu_1\partial_{x_2}v_2.$$

Hence, we get

$$\int_{\Lambda_R}(\nabla\cdot\boldsymbol{u})(\nabla\cdot\bar{\boldsymbol{v}})(\boldsymbol{\nu}\cdot\boldsymbol{p})\,\mathrm{d}s=\int_{\Lambda_R}(\nabla\cdot\boldsymbol{u})(\boldsymbol{\nu}\cdot(\boldsymbol{p}\cdot\nabla\bar{\boldsymbol{v}}))\,\mathrm{d}s.$$

Combining the above identities gives

$$\begin{aligned}g_2(\boldsymbol{p})(\boldsymbol{u},\boldsymbol{v})=&(\lambda+\mu)\int_{\Omega_R}(\nabla\cdot\boldsymbol{u})\nabla\cdot(\boldsymbol{p}\cdot\nabla\bar{\boldsymbol{v}})\,\mathrm{d}\boldsymbol{x}+(\lambda+\mu)\int_{\Omega_R}\nabla\cdot(\boldsymbol{p}\cdot\nabla\boldsymbol{u})(\nabla\cdot\bar{\boldsymbol{v}})\,\mathrm{d}\boldsymbol{x}\\&-(\lambda+\mu)\int_{\Lambda_R}(\nabla\cdot\boldsymbol{u})(\boldsymbol{\nu}\cdot(\boldsymbol{p}\cdot\nabla\bar{\boldsymbol{v}}))\,\mathrm{d}s.\end{aligned}\tag{4.12}$$

Noting (4.10), and adding (4.11) and (4.12), we obtain

$$\begin{aligned}b(\dot{\boldsymbol{u}},\boldsymbol{v})=&\mu\int_{\Omega_R}\nabla(\boldsymbol{p}\cdot\nabla\boldsymbol{u}):\nabla\bar{\boldsymbol{v}}\,\mathrm{d}\boldsymbol{x}+(\lambda+\mu)\int_{\Omega_R}\nabla\cdot(\boldsymbol{p}\cdot\nabla\boldsymbol{u})(\nabla\cdot\bar{\boldsymbol{v}})\,\mathrm{d}\boldsymbol{x}\\&-\omega^2\int_{\Omega_R}(\boldsymbol{p}\cdot\nabla\boldsymbol{u})\cdot\bar{\boldsymbol{v}}\,\mathrm{d}\boldsymbol{x}.\end{aligned}$$

Define $\boldsymbol{u}'=\dot{\boldsymbol{u}}-\boldsymbol{p}\cdot\nabla\boldsymbol{u}$. It is clear to note that $\boldsymbol{p}\cdot\nabla\boldsymbol{u}=0$ on S_R since $\boldsymbol{p}=0$ on S_R. Hence, we have

$$b(\boldsymbol{u}',\boldsymbol{v})=0,\quad\forall\boldsymbol{v}\in H^1_{\Lambda_R}(\Omega_R)^2,\tag{4.13}$$

which shows that $\boldsymbol{u}'$ is the weak solution of the boundary value problem (4.8). To verify the boundary condition of $\boldsymbol{u}'$ on S_R, we recall the definition of $\boldsymbol{u}'$ and have

$$\boldsymbol{u}'=\lim_{h\to0}\frac{\breve{\boldsymbol{u}}-\boldsymbol{u}}{h}-\boldsymbol{p}\cdot\nabla\boldsymbol{u}=-\boldsymbol{p}\cdot\nabla\boldsymbol{u}\quad\text{on }\Lambda_R,$$

since $\breve{\boldsymbol{u}}=\boldsymbol{u}=0$ on Λ_R. Noting that $\boldsymbol{u}=0$ and thus $\partial_{\boldsymbol{\tau}}\boldsymbol{u}=0$ on Λ_R, we have

$$\boldsymbol{p}\cdot\nabla\boldsymbol{u}=(\boldsymbol{p}\cdot\boldsymbol{\nu})\partial_{\boldsymbol{\nu}}\boldsymbol{u}+(\boldsymbol{p}\cdot\boldsymbol{\tau})\partial_{\boldsymbol{\tau}}\boldsymbol{u}=(\boldsymbol{p}\cdot\boldsymbol{\nu})\partial_{\boldsymbol{\nu}}\boldsymbol{u},\tag{4.14}$$

which completes the proof by combining (4.13) and (4.14). ∎

4.2. Reconstruction method. Denote by Λ_N the approximation of the locally perturbed surface Λ_R, where

$$\Lambda_N=\{(x_1,x_2)\in\mathbb{R}^2:x_2=f_N(x_1),|x_1|<R\},$$

and

$$f_N(x)=\sum_{i=1}^{N}c_iB_i^3(x).$$

Here $\{B_i^3\}$ are third order B-splines with uniformly distributed nodes $\{t_i\}$ in $[-R,R]$. To reconstruct the locally perturbed surface, it suffices to determine the coefficients c_i.

Let Ω_N be the domain bounded by Λ_N and S_R. Denote a vector of coefficients $\boldsymbol{C}=(c_1,...,c_N)^\top\in\mathbb{R}^N$, and a vector of measurement data $\boldsymbol{U}=(\boldsymbol{u}(\boldsymbol{x}_1),...,\boldsymbol{u}(\boldsymbol{x}_M))^\top\in\mathbb{C}^{2M}$, where $\boldsymbol{x}_m\in S_R,m=1,...,M$. The inverse problem can be formulated to solve an approximate nonlinear equation

$$\mathcal{F}_N(\boldsymbol{C})=\boldsymbol{U},$$

where the operator $\mathcal{F}_N$ maps a vector in $\mathbb{R}^N$ into another vector in $\mathbb{C}^{2M}$.

The following theorem is a direct conclusion of Theorem 4.1.

THEOREM 4.2. *Let $\boldsymbol{u}_N$ be the solution of the variational problem (3.5) with the locally perturbed surface Λ_N. The operator $\mathcal{F}_N$ is differentiable and its derivatives are given by*

$$\frac{\partial \mathcal{F}_{N,m}(\boldsymbol{C})}{\partial c_n} = \boldsymbol{u}_n'(\boldsymbol{x}_m), \qquad n=1,...,N; m=1,..,M,$$

where $\boldsymbol{u}_n'$ is the unique weak solution of the boundary value problem

$$\begin{cases} \mu\Delta \boldsymbol{u}_n' + (\lambda+\mu)\nabla\nabla\cdot \boldsymbol{u}_n' + \omega^2 \boldsymbol{u}_n' = 0 & \text{in } \Omega_N, \\ \boldsymbol{u}_n' = -(\boldsymbol{p}_n\cdot\boldsymbol{\nu})\partial_{\boldsymbol{\nu}}\boldsymbol{u}_N & \text{on } \Lambda_N, \\ \mu\partial_{\boldsymbol{\nu}}\boldsymbol{u}_n' + (\lambda+\mu)(\nabla\cdot\boldsymbol{u}_n')\boldsymbol{\nu} = \mathcal{A}\boldsymbol{u}_n' & \text{on } S_R. \end{cases} \tag{4.15}$$

Here $\boldsymbol{p}_n(x_1) = (x_1, B_n^3(x_1))^\top$.

We remark that, since S_R is C^∞-smooth and the boundary condition on S_R is non-local, the weak solution to (4.15) is C^∞-smooth up to the boundary S_R by standard elliptic interior estimate. Therefore, the values of $\boldsymbol{u}_n'$ at $\boldsymbol{x}_m$ are all well-defined.

The inverse problem can be formulated as the minimization problem:

$$\min_{\mathbf{C}} q(\mathbf{C}), \qquad \mathbf{C}\in\mathbb{R}^N,$$

where the cost function is defined as

$$q(\boldsymbol{C}) = \frac{1}{2}||\mathcal{F}_N(\mathbf{C}) - \boldsymbol{U}||^2 = \frac{1}{2}\sum_{m=1}^{M} |\mathcal{F}_{N,m}(\mathbf{C}) - \boldsymbol{u}(\boldsymbol{x}_m)|^2.$$

By using Theorem 4.2, we have, from a simple calculation, that

$$\nabla q(\mathbf{C}) = \left(\frac{\partial q(\mathbf{C})}{\partial c_1}, ..., \frac{\partial q(\mathbf{C})}{\partial c_N}\right)^\top,$$

where

$$\frac{\partial q(\mathbf{C})}{\partial c_n} = \mathrm{Re}\sum_{m=1}^{M} \boldsymbol{u}_n'(\boldsymbol{x}_m)\cdot(\bar{\mathcal{F}}_{N,m}(\mathbf{C}) - \bar{\boldsymbol{u}}(\boldsymbol{x}_m)).$$

We assume that the scattering data $\mathbf{U}$ is available over a range of angular frequencies $\omega\in[\omega_{\min},\omega_{\max}]$, which may be divided into $\omega_{\min}=\omega_0<\omega_1<\cdots<\omega_K=\omega_{\max}$. Correspondingly, the compressional wavenumber may be divided into $\kappa_{1,\min}=\kappa_{1,0}<\kappa_{1,1}<\cdots<\kappa_{1,K}=\kappa_{1,\max}$ and the shear wavenumber may be divided into $\kappa_{2,\min}=\kappa_{2,0}<\kappa_{2,1}<\cdots<\kappa_{2,K}=\kappa_{2,\max}$.

We now propose an algorithm to reconstruct the coefficients c_i, $i=1,...,N$.

(1) Set an trivial initial approximation: $c_j=0, j=1,...,N$, i.e., the initial approximation is a flat surface.

(2) Begin with the smallest frequency ω_0, and seek an approximation to the functions f_N by B-Splines with N number of uniformly distributed nodes in $[-R,R]$.

$$f_{k_0} = \sum_{i=1}^{N} c_i^0 B_i^3(x).$$

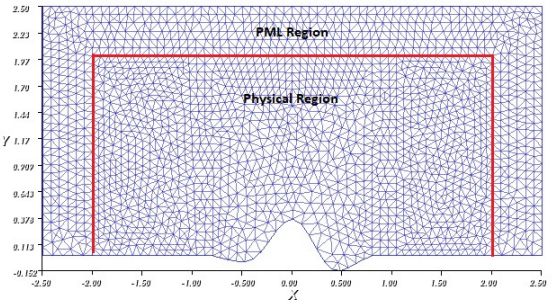

FIG. 5.1. *A typical diagram of the computational domain for PML problem.*

Denote $\mathbf{C}_{k_0}=(c_1,c_2,\ldots,c_N)^\top$ and consider the iteration

$$\mathbf{C}_{k_0}^{(l+1)}=\mathbf{C}_{k_0}^{(l)}-\varepsilon\nabla q(\mathbf{C}_{k_0}^{(l)}),\quad l=1,\ldots,L,$$

where $\varepsilon>0$ and $L>0$ are the step size and the number of iterations for a fixed frequency, respectively.

(3) Increase to the next higher frequency ω_1 of the available data. Repeat Step 2 with the previous approximation to f_N as the starting point.

(4) Repeat Step 3 until a prescribed highest frequency ω_K is reached.

5. Numerical experiments

5.1. Forward problem. The scattering data is obtained by using the finite element method with the Perfectly Matched Layer (PML) technique in a locally perturbed half-plane, which is implemented via Freefem++ [17]. The forward scattering problem can be equivalently formulated as the following boundary value problem

$$\begin{aligned}\mu\Delta\boldsymbol{v}+(\lambda+\mu)\nabla\nabla\cdot\boldsymbol{v}+\omega^2\boldsymbol{v}=0\quad&\text{in }\Omega,\\ \boldsymbol{v}=-\boldsymbol{u}_0\quad&\text{on}\quad\Gamma_f,\end{aligned}\tag{5.1}$$

where $\boldsymbol{v}=[v_1,v_2]^\top$ satisfies the outgoing Sommerfeld radiation condition in Ω and $\boldsymbol{u}_0$ is the reference field. The physical domain of interest is

$$\Omega_a:=\Omega\cap\{x:-a\le x_1\le a, f(x_1)\le x_2\le a\}$$

for some $a>R$, which contains the semi-circle S_R. Here the function $f(x_1)$ depicts the profile. We introduce an absorbing layer of width L and pose a boundary value problem in the computational domain Ω_{a+L}, as shown in Figure 5.1. We note that, since $\boldsymbol{v}=\boldsymbol{u}_0=0$ on $\{(x_1,0):a<|x_1|<a+L\}$, the truncation of the physical domain in the x_1-direction does not give rise to truncation errors in our numerical scheme. Let $s_1(x_1)=1+\mathrm{i}\sigma_1(x_1), s_2(x_2)=1+\mathrm{i}\sigma_2(x_2)$ be the absorbing medium property, where σ_1 and σ_2 are positive continuous functions satisfying $\sigma_1=\sigma_2=0$ in the physical domain. Then the forward scattering data are obtained by numerically solving the following PML-equations in the computational domain Ω_{a+L}:

$$(\lambda+2\mu)\partial_1(\frac{s_2}{s_1}\partial_1 v_1)+\mu\partial_2(\frac{s_1}{s_2}\partial_2 v_1)+(\lambda+\mu)\partial_{1,2}^2 v_2+s_1s_2\omega^2v_1=0,$$

$$\mu\partial_1(\frac{s_2}{s_1}\partial_1 v_2)+(\lambda+2\mu)\partial_2(\frac{s_1}{s_2}\partial_2 v_2)+(\lambda+\mu)\partial_{1,2}^2 v_1+s_1 s_2\omega^2 v_2=0,$$

together with the Dirichlet boundary conditions

$$\boldsymbol{v}=-\boldsymbol{u}_0 \quad \text{on} \quad \Gamma_f\cap\{x:|x_1|<a\}, \qquad \boldsymbol{v}=0 \quad \text{on} \quad \Gamma^{\mathrm{PML}},$$

where $\Gamma^{\mathrm{PML}}=\partial\Omega_{a+L}\setminus(\Gamma_f\cap\{x:|x_1|<a\})$.

5.2. Inverse problem. In this section, we present three examples to show the results of the inversion scheme proposed in Section 4. The finite element solution obtained by PML-scheme is interpolated uniformly to get the near-field data measured on S_R. To test the stability, we add an amount of relative noise to the data

$$\boldsymbol{u}^\delta(\boldsymbol{x}_i)=\boldsymbol{u}(\boldsymbol{x}_i)(1+\delta\,\mathrm{rand}), \quad i=1,\dots,M,$$

where rand are uniformly distributed random numbers in $[-1,1]$.

In the following three examples, we take the Lamé constants $\lambda=2,\mu=1$, which account for the compressional wavenumber $\kappa_1=\omega/2$. The incident wave is taken as a single compressional wave at normal incidence, i.e. $\boldsymbol{u}^{\mathrm{in}}=[0,1]e^{-\mathrm{i}\kappa_1 y}$. The radius of the half-circle B_R^+ is $R=1$, and the total number of measurement points are $M=100$. The noise level of measurement is $\delta=5\%$. We take the scattering data at nine frequencies $\omega_i=2i+3, i=1,2..,9$, and the corresponding compressional wave number is $\kappa_{1,i}=2.5,3.5,...,10.5$. For fixed angular frequency $\omega_i=2i+3$ in each iteration, the total number of iterations is $10+i$ with step size $0.0005/i$.

Example 1. Consider a locally perturbed surface with two separated upward parts represented by

$$f(x_1)=\begin{cases}0.1+0.1\cos(4\pi(x_1+0.15)+\pi), & x_1\in[-0.65,-0.15),\\ 0.05+0.05\cos(4\pi(x_1-0.15)+\pi), & x_1\in[0.15,0.65],\\ 0, & \text{otherwise.}\end{cases}$$

It is expected that our method works very well even by using only a few scattering data. We use only a single compressional plane wave at normal incidence to illuminate the surface. Figure 5.3 shows the numerical results, where the computed scattering surface (dot-dashed line) is plotted against the exact surface (dashed line) for different data apertures(solid line). Figure 5.3(a) shows the exact surface and the initial guess of the flat surface. Figure 5.3(b) shows the reconstructed surface by using the full aperture data, i.e., the observation angle $\psi\in[0,\pi]$. The result is perfect. Figure 5.3(c) shows how the maximal frequency influences the quality of the reconstruction. Figure 5.3(c) shows that if we use lower maximal frequency, i.e., $\omega=5,..,13$, the main feature of the surface can be recovered, but the small details can not be reconstructed unless higher maximal frequency is used. We also investigate how the data aperture influences the quality of the reconstruction. Figures 5.3(d)-(e) plot the reconstructed surfaces and the corresponding data aperture for the construction. We choose the observation angle $\psi\in[0.5\pi,\pi]$ in Figure 5.3(d), and $\psi\in[0.25\pi,\pi]$ in Figure 5.3(e). It can be clearly noted that the part of the surface can be accurately reconstructed as long as it can be seen, i.e., the observation angles can cover that part. Finally, Figure 5.3(f) shows the result by using a single frequency $\omega=21$. It can be clearly noted that the result converges to a local minimum which is far away from true surface. This illustrates the importance of using continuation technique.

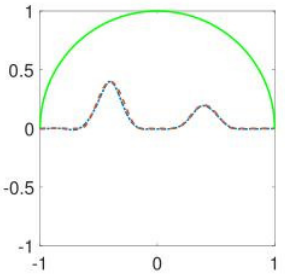

FIG. 5.2. *Reconstruction of a surface with a height of 0.4.*

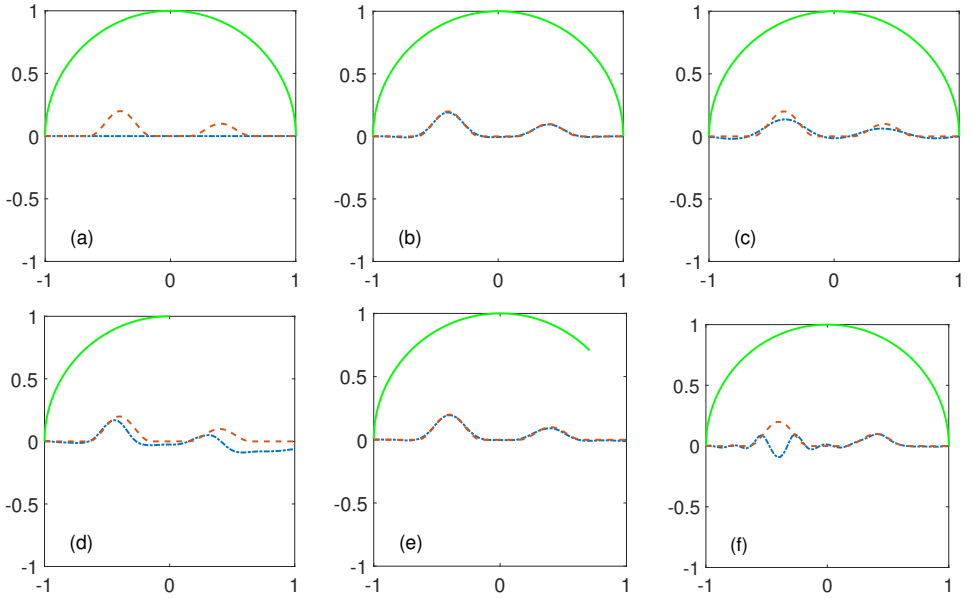

FIG. 5.3. *example 1: two upward surfaces. computed (dot-dashed line) against exact (dashed line). (a) exact surface and initial guess of the flat surface; (b)* $\psi \in [0,\pi]$*; (c)* $\psi \in [0,\pi]$ *with* $\omega = 5,\ldots,13$*; (d)*$\psi \in [\pi/2,\pi]$*; (e)* $\psi \in [\pi/4,\pi]$*; (f) reconstruction from a single frequency* $\omega = 21$.

It can be seen from Figure 5.2 that a locally perturbed surface with a relatively large height of 0.4 can be also well-reconstructed.

Example 2. Consider a locally perturbed surface with both upward and downward parts represented by

$$f(x_1) = \begin{cases} 0.1 + 0.1\cos(4\pi(x_1 + 0.15) + \pi), & x_1 \in [-0.65, -0.15), \\ -0.05 - 0.05\cos(4\pi(x_1 - 0.15) + \pi), & x_1 \in [0.15, 0.65], \\ 0, & \text{otherwise.} \end{cases}$$

Due to the upward and downward feature, this surface is more difficult than the first example. We use only a single compressional plane wave at normal incidence to illuminate the surface. Figure 5.4(a) shows the exact surface and the initial guess of the

flat surface. Figure 5.4(b) shows the reconstructed surface by using the full aperture data, i.e., the observation angle $\psi \in [0,\pi]$. Figure 5.4(c) shows the result by using lower maximal frequency, i.e., $\omega = 5,..,13$. Figures 5.4(d)-(e) plot the reconstructed surfaces and the corresponding data aperture for the construction. We obtain that the part of the surface can be accurately reconstructed as long as it can be seen, i.e., the observation angles can cover that part. Finally, Figure 5.4(f) shows the result by using a single frequency $\omega = 21$.

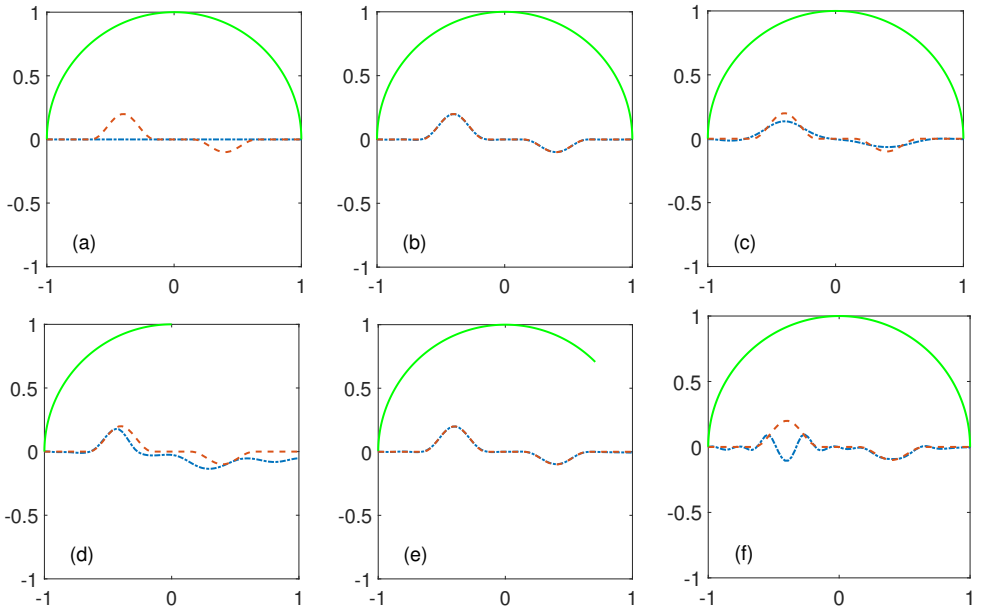

FIG. 5.4. *example 2: upward and downward surface. computed (dot-dashed line) against exact (dashed line). (a) exact surface and initial guess of the flat surface; (b) $\psi \in [0,\pi]$; (c) $\psi \in [0,\pi]$ with $\omega = 5,...,13$; (d)$\psi \in [\pi/2,\pi]$; (e) $\psi \in [\pi/4,\pi]$; (f) reconstruction from a single frequency $\omega = 21$.*

Example 3. Consider a locally perturbed surface with two separated downward parts represented by

$$f(x_1) = \begin{cases} -0.1 - 0.1\cos(4\pi(x_1 + 0.15) + \pi), & x_1 \in [-0.65, -0.15), \\ -0.05 - 0.05\cos(4\pi(x_1 - 0.15) + \pi), & x_1 \in [0.15, 0.65], \\ 0, & \text{otherwise.} \end{cases}$$

Due to the two downward feature, our problem is equivalent to a multi-cavity scattering problem. We use only a single compressional plane wave at normal incidence to illuminate the surface. Figure 5.5(a) shows the exact surface and the initial guess of the flat surface. Figure 5.5(b) shows the reconstructed surface by using the full aperture data, i.e., the observation angle $\psi \in [0,\pi]$. Figure 5.5(c) shows the result by using lower maximal frequency, i.e., $\omega = 5,..,13$. Figures 5.5(d)-(e) plot the reconstructed surfaces and the corresponding data aperture for the construction. We obtain that the part of the surface can be accurately reconstructed as long as it can be seen, i.e., the observation angles can cover that part. Finally, Figure 5.5(f) shows the result by using a single frequency $\omega = 21$.

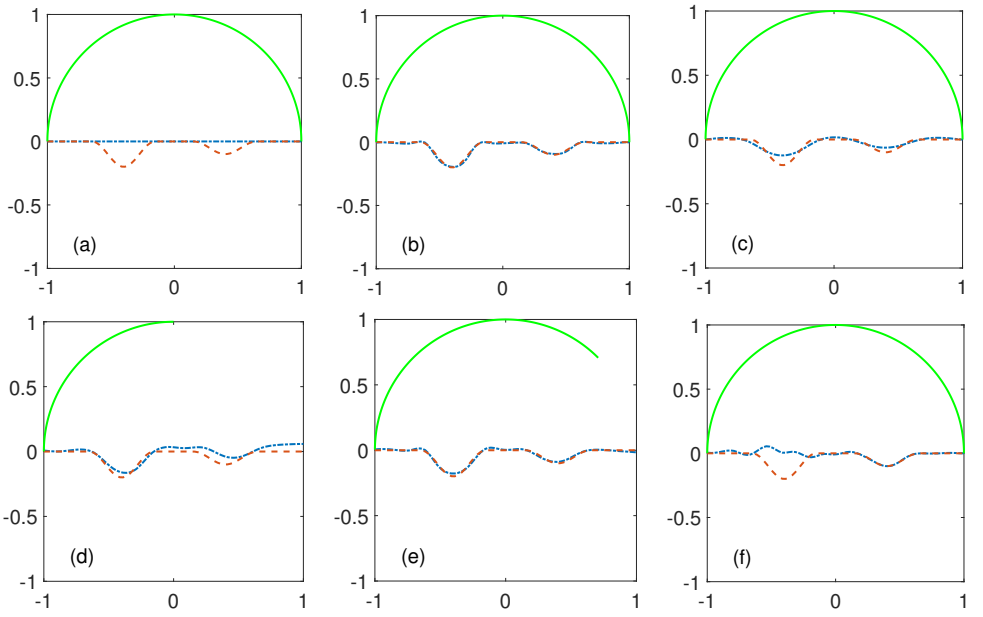

FIG. 5.5. *Example 3: the two downward profile. computed (dot-dashed line) against exact (dashed line). (a) exact surface and initial guess of the flat surface; (b)* $\psi \in [0,\pi]$*; (c)* $\psi \in [0,\pi]$ *with* $\omega = 5,...,13$*; (d)*$\psi \in [\pi/2,\pi]$*; (e)* $\psi \in [\pi/4,\pi]$*; (f) reconstruction from a single frequency* $\omega = 21$.

Example 4. Consider a multiscale surface represented by

$$f(x_1) = \begin{cases} 0.13 + 0.1\cos((4/3)\pi x_1) + 0.03\cos((16/3)\pi x_1 + \pi), & x_1 \in [-0.75, 0.75], \\ 0, & \text{otherwise}, \end{cases}$$

This surface has two scales. The macro-scale part of the surface is a cos function with period 1.5 and the micro-scale part is a perturbation by cos function with smaller period $\frac{3}{8}$. This example illustrates that the macro-scale part can be reconstructed by using low frequency, but the micro-scale part can only be reconstructed with high frequency. Figure 5.6(a) shows the exact surface and the initial guess of the flat surface. Figure 5.6(b) shows the reconstructed surface by using the full aperture data, i.e., the observation angle $\psi \in [0,\pi]$. Figure 5.6(c) shows the result by using lower maximal frequency, i.e., $\omega = 5,..,13$. Figures 5.6(d)-(e) plot the reconstructed surfaces and the corresponding data aperture for the construction. We obtain that the part of the surface can be accurately reconstructed as long as it can be seen, i.e., the observation angles can cover that part. Finally, Figure 5.6(f) shows the result by using a single frequency $\omega = 21$.

Our inversion scheme requires an efficient forward solver to compute the domain derivative problem. In fact, we need to compute N times the solution u_n' of (4.15) and one time the total field $\bar{u}$ that corresponds to the current approximated surface. Multiplying them with the number of iterations gives the compuational cost of our method. Since the descent method for most time is of first order, we need many iterations in order to get a good approximation. The larger the height of the surface, the more the number of the iterations. This means that the number of direct problems to be solved is quite large. However, since the main computational efforts are spent on the calcula-

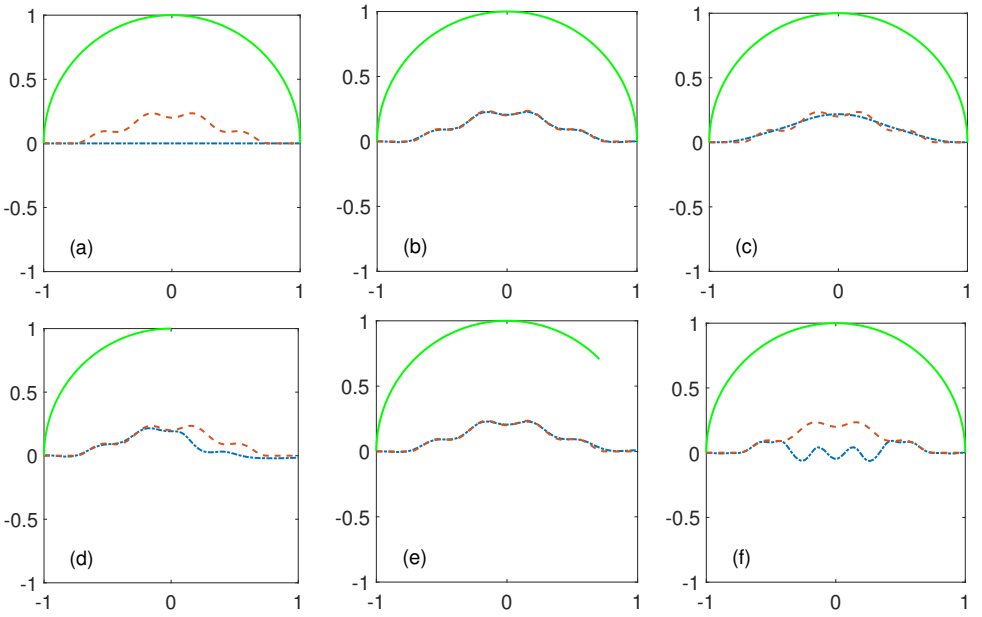

FIG. 5.6. *example 4: multiscale surface. computed (dot-dashed line) against exact (dashed line). (a) exact surface and initial guess of the flat surface; (b)* $\psi \in [0, \pi]$*; (c)* $\psi \in [0, \pi]$ *with* $\omega = 5, ..., 13$*; (d)*$\psi \in [\pi/2, \pi]$*; (e)* $\psi \in [\pi/4, \pi]$*; (f) reconstruction from a single frequency* $\omega = 21$.

tion of u_n', the total cost can be reduced by parallel schemes with enough computing cores. Let us also mention that our continuation approach using multi-frequencies does not require a good initial guess. In our examples, two upward surfaces, upward and downward surfaces, two downward surfaces as well as multiscale surfaces can be almost perfectly reconstructed from the initial guess of the unperturbed flat surface. This is the advantage of our proposed method.

6. Concluding remarks

In this paper we have proved well-posedness of time-harmonic elastic scattering from a locally perturbed rigid rough surface in 2D. Thanks to the Dirichlet Green's tensor in a half-plane, we have established an equivalent variational formulation in a truncated bounded domain coupled with a transparent boundary condition derived from the integral representation of the scattered field. Our studies show that, due to the presence of a local perturbation, both analysis and numerics for rough surface scattering problems can be significantly simplified. This enables us to deeply interpret the perturbed wave modes scattered back into the upper half-plane. An iterative continuation method was proposed for reconstructing the unknown interface by applying the domain derivative formula. Extension of these works to 3D requires analysis of the Green's tensor in a half-space and an efficient algorithm for the direct scattering problem. This paper also provides insight into the more practical problems under the traction-free boundary condition. Further, the direct and inverse problems for general rough surfaces are challenging. Progress in these directions will be reported in our forthcoming publications.

Acknowledgements. The work of G. Hu is supported by the NSFC grant (No. 11671028) and NSAF grant (No. U1530401).

REFERENCES

[1] I. Abubakar, *Scattering of plane elastic waves at rough surface I*, Proc. Cambridge Philos. Soc., 58:136–157, 1962. 1

[2] J.D. Achenbach, *Wave Propagation in Elastic Solids*, North Holland, Amsterdam, 1973. 1

[3] T. Arens, *The scattering of elastic waves by rough surfaces*, PhD thesis, Brunel University, June 2000. 3

[4] T. Arens, *Uniqueness for elastic wave scattering by rough surfaces*, SIAM J. Math. Anal., 33:461–476, 2001. 1, 3, 3

[5] T. Arens, *Existence of solution in elastic wave scattering by unbounded rough surfaces*, Math. Meth. Appl. Sci., 25:507–528, 2002. 1, 3

[6] H. Ammari, G. Bao, and A.Wood, *An integral equation method for the electromagnetic scattering from cavities*, Math. Meth. Appl. Sci., 23:1057–1072, 2000. 1

[7] H. Ammari, G. Bao, and A.W. Wood, *Analysis of the electromagnetic scattering from a cavity*, Japan J. Indust. Appl. Math., 19:301–310, 2002. 1

[8] G. Bao, J. Gao, and P. Li, *Analysis of direct and inverse cavity scattering problems*, Numer. Math. Theor. Meth. Appl., 4:419–442, 2011. 1

[9] G. Bao, G. Hu, and T. Yin, *Time-harmonic acoustic scattering from locally perturbed half-planes*, SIAM J. Appl. Math., 78:2672-2691, 2018. 1

[10] G. Bao and J. Lin, *Imaging of local surface displacement on an infinite ground plane: The multiple frequency case*, SIAM J. Appl. Math., 71:1733–1752, 2011. 1

[11] G. Bao and J. Lin, *Imaging of reflective surfaces by near-field optics*, Optics Letters, 37:5027–5029, 2012. 1

[12] S.N. Chandler-Wilde and P. Monk, *Existence, uniqueness and variational methods for scattering by unbounded rough surfaces*, SIAM J. Math. Anal., 37:598–618, 2015. 1, 2

[13] A. Charalambopoulos, *On the Fréchet differentiability of boundary integral operators in the inverse elastic scattering problem*, Inverse Problems, 11:1137–1161, 1995. 1

[14] J. Elschner and G. Hu, *Elastic scattering by unbounded rough surfaces*, SIAM J. Math. Anal., 44:4101–4127, 2012. 1, 2, 3

[15] J. Elschner and G. Hu, *Variational approach to scattering of plane elastic waves by diffraction gratings*, Math. Meth. Appl. Sci., 33:1924–1941, 2010. 1

[16] J. Elschner and G. Hu, *Scattering of plane elastic waves by three-dimensional diffraction gratings*, Math. Models Meth. Appl. Sci., 22:1150019, 2012. 1

[17] F. Hecht, *New development in FreeFem++*, J. Numer. Math., 20:251–265, 2012. 5.1

[18] F. Hettlich, *Fréchet derivative in inverse obstacle scattering*, Inverse Problems, 11:371–382, 1995. 1

[19] G.C. Hsiao and W.L. Wendland, *Boundary Integral Equations*, Springer, Berlin, 2008. 1

[20] J.M. Jin, *Electromagnetic scattering from large, deep, and arbitrarily-shaped open cavities*, Electromagnetics, 18:3–34, 1998. 1

[21] A. Kirsch, *The domain derivative and two applications in inverse scattering theory*, Inverse Problems, 9:81–96, 1993. 1

[22] Kupradze VD et al., *Three-dimensional Problems of the Mathematical Theory of Elasticity and Thermoelasticity*, North-Holland, Amsterdam, 1979. 3

[23] F. Le Loüer, *On the Fréchet derivative in elastic obstacle scattering*, SIAM J. Appl. Math., 72:1493–1507, 2012. 1

[24] P. Li, Y. Wang, and Y. Zhao, *Inverse elastic surface scattering near-field data*, Inverse Problems, 31:035009, 2015. 1

[25] P. Li, *An inverse cavity problem for Maxwell's equations*, J. Diff. Eqs., 252:3209–3225, 2012. 1

[26] P. Li, *Coupling of finite element and boundary integral methods for electromagnetic scattering in a two-layered medium*, J. Comput. Phys., 229:481–497, 2010. 1

[27] P. Li, *A survey of open cavity scattering problems*, J. Comp. Math., 36(1):1–16, January 2018. 1

[28] P. Li, H. Wu, and W. Zheng, *An overfilled cavity problem for Maxwell's equations*, Math. Meth. Appl. Sci., 35:1951–1979, 2012. 1

[29] W. Mclean, *Strongly Elliptic Systems and Boundary Integral Equations*, Cambridge University Press, Cambridge, 2010. 2, 3

[30] R. Potthast, *Domain derivatives in electromagnetic scattering*, Math. Meth. Appl. Sci., 19:1157–1175, 1996. 1

[31] J.W.C. Sherwood, *Elastic wave propagation in a semi-infinite solid medium*, Proc. Phys. Soc., 71:207–219, 1958. 1

[32] A. Willers, *The Helmholtz equation in disturbed half-spaces*, Math. Meth. Appl. Sci., 9:312–323, 1987. 1

[33] A. Wood, *Analysis of electromagnetic scattering from an overfilled cavity in the ground plane*, J.

Comput. Phys., 215:630–641, 2006. 1

[34] H. Zhang and B. Zhang, *A novel integral equation for scattering by locally rough surface and applications to the inverse problem*, SIAM J. Appl. Math., 73:1811–1829, 2013. 1